

# Measurement of diffuse gamma-ray emission from Galactic plane with LHAASO

Qiang Yuan

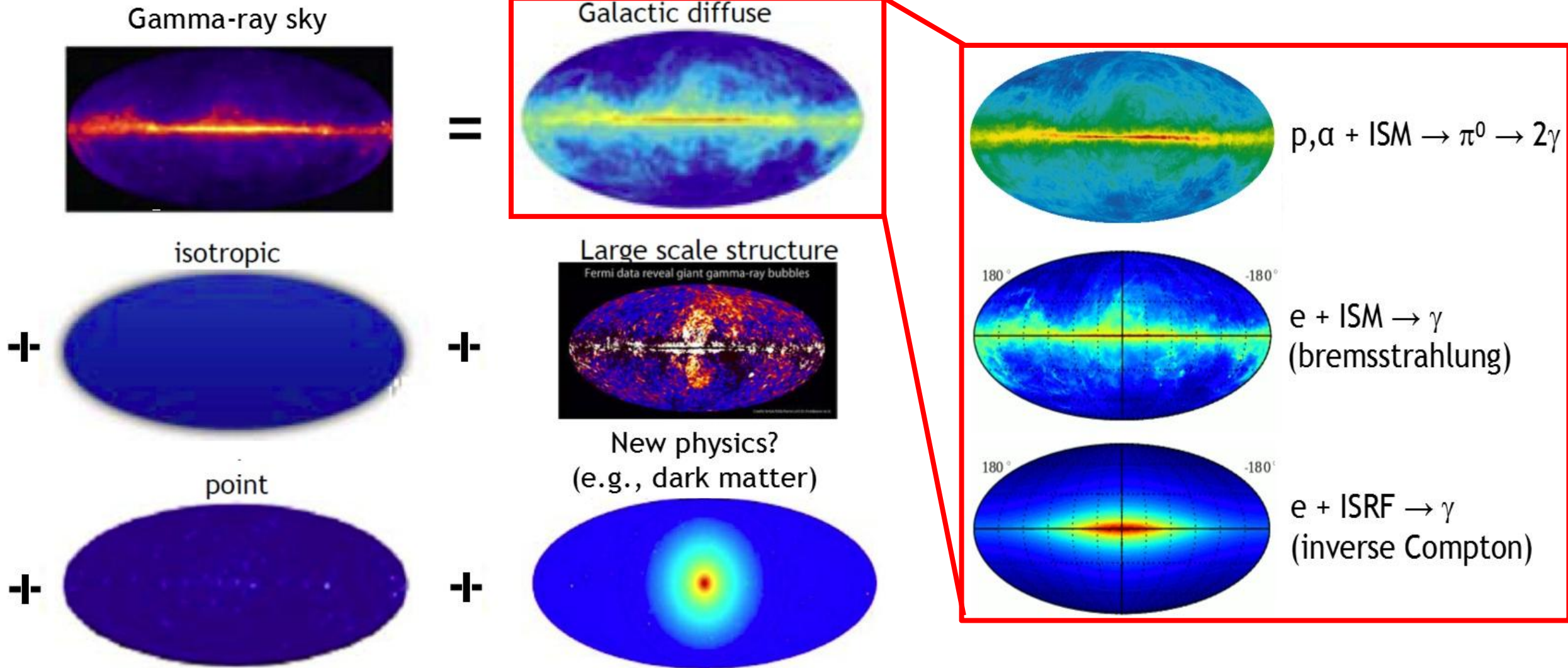
on behalf of the LHAASO collaboration

Purple Mountain Observatory, Chinese Academy of Science

(2023, PRL, 131, 151001; 2025, PRL, 134, 081002)

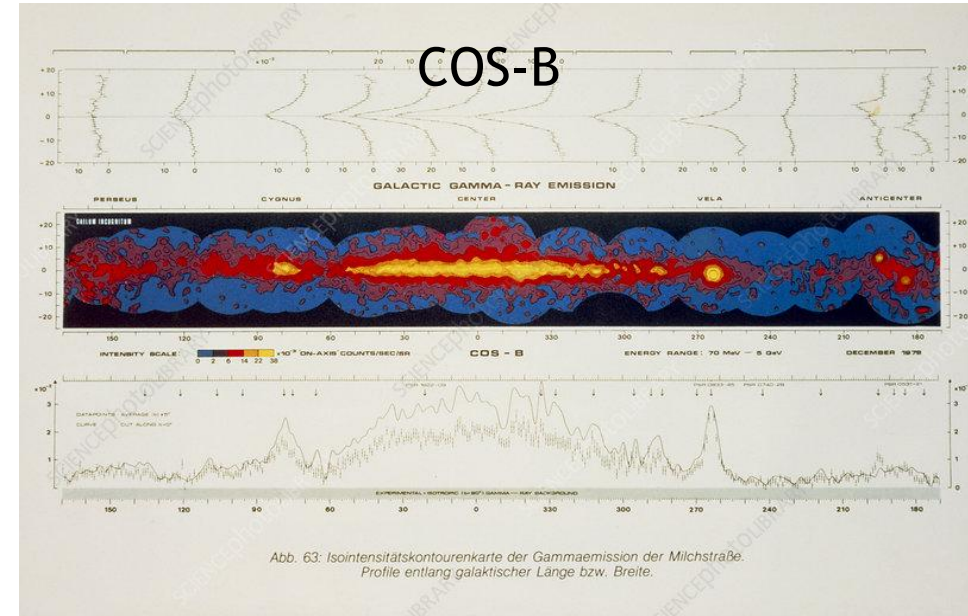
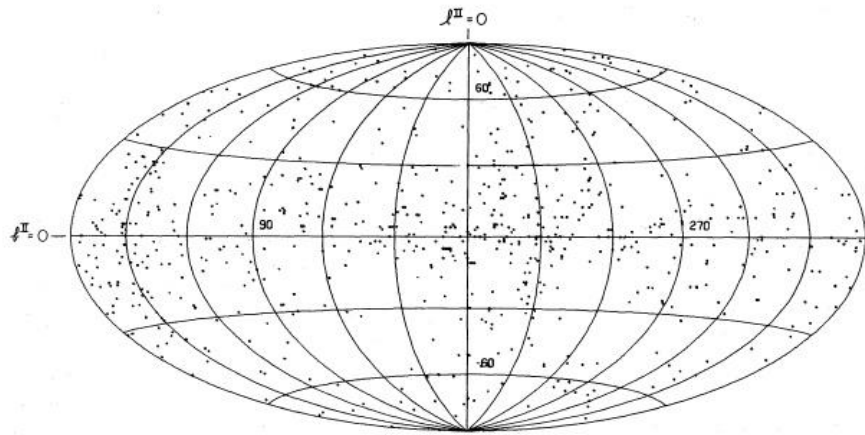
The 2nd LHAASO Symposium, Hongkong, China, Mar. 21-25, 2025

# The gamma-ray sky

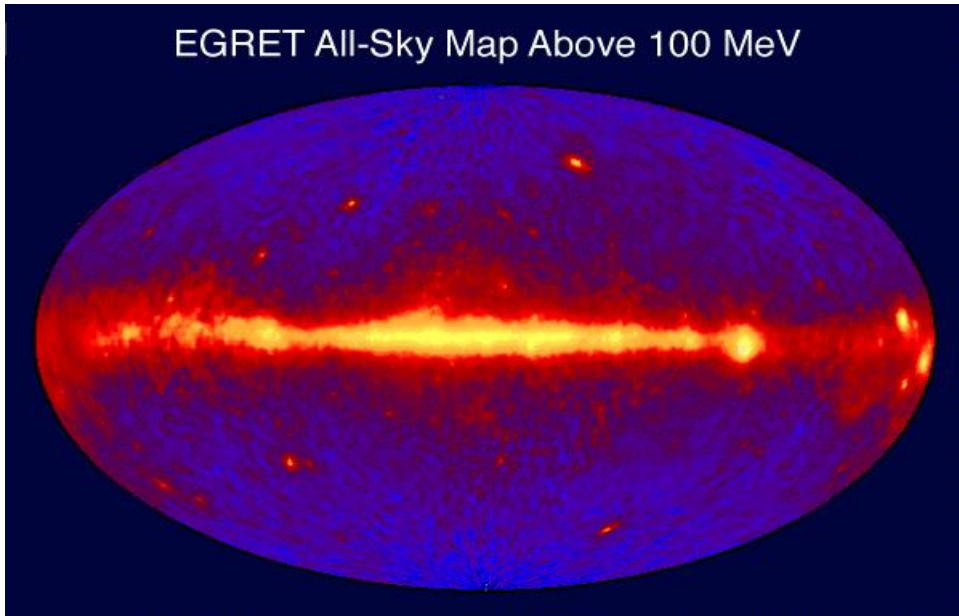


# Diffuse $\gamma$ -ray observations from space (<TeV)

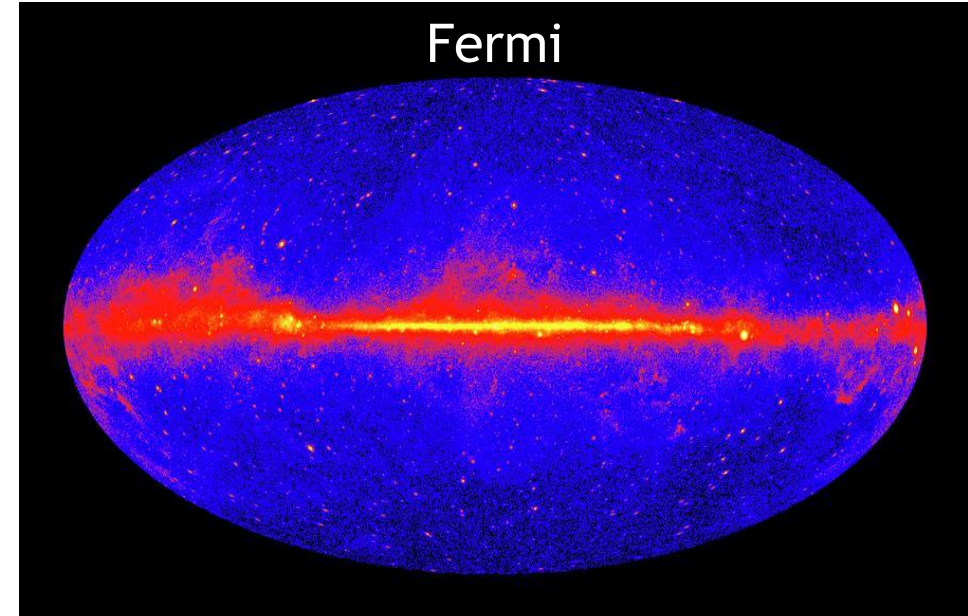
OSO-3: 621 gamma-rays



EGRET All-Sky Map Above 100 MeV

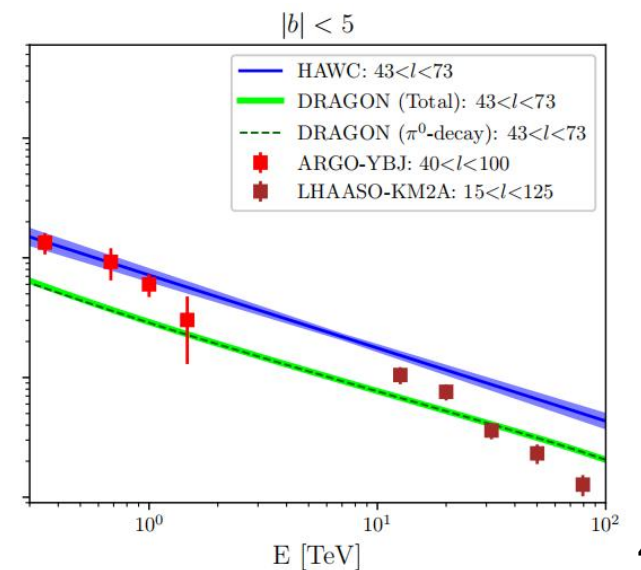
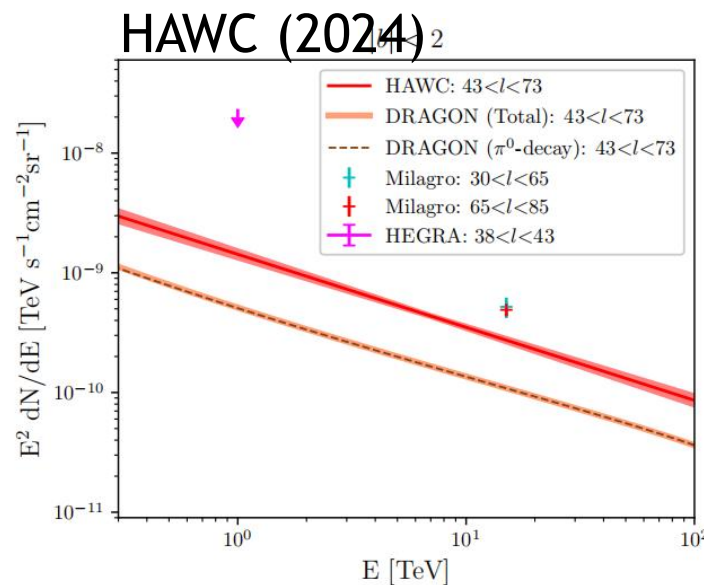
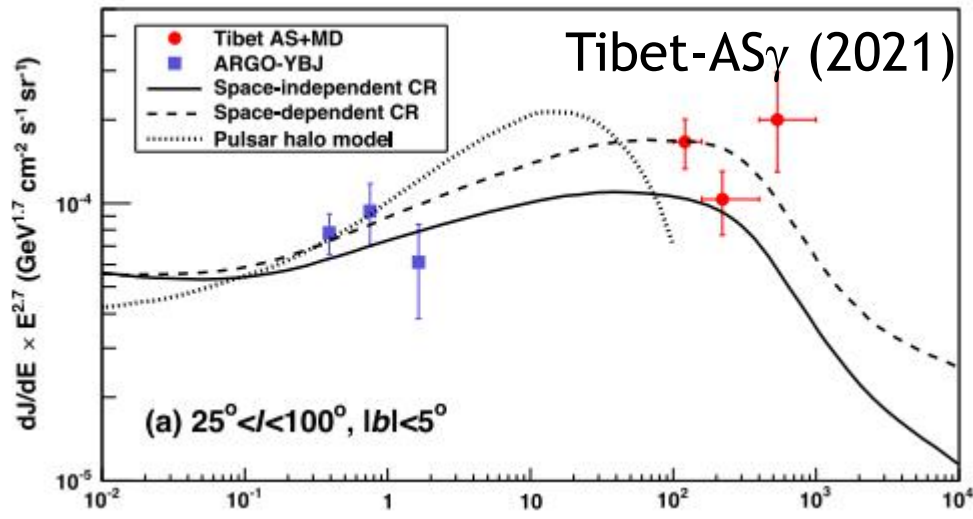
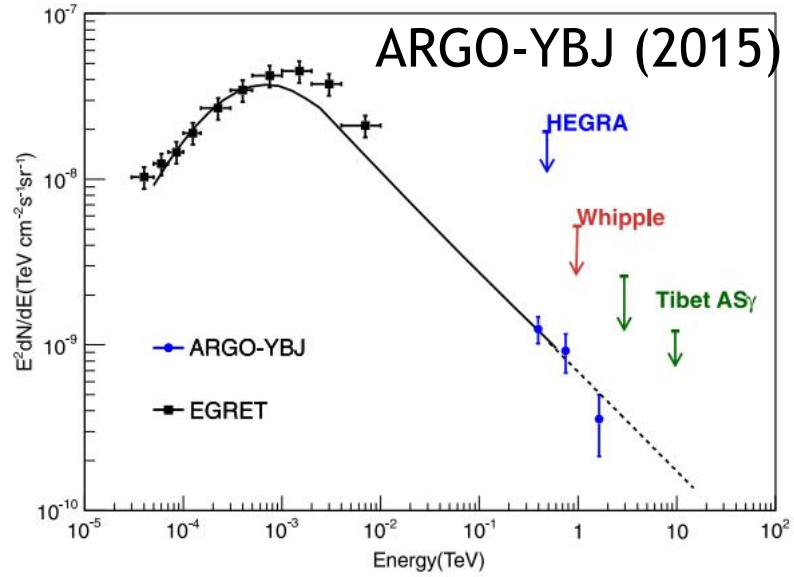
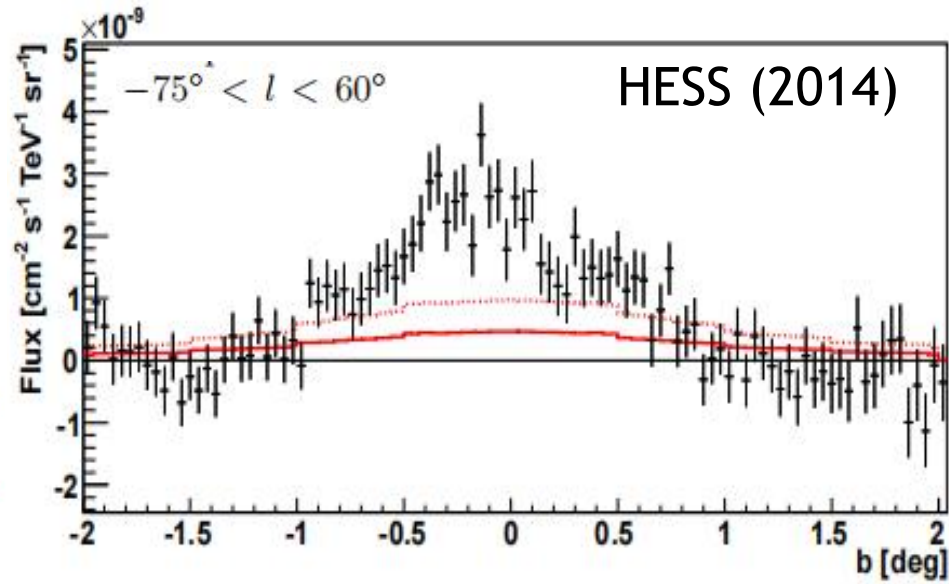
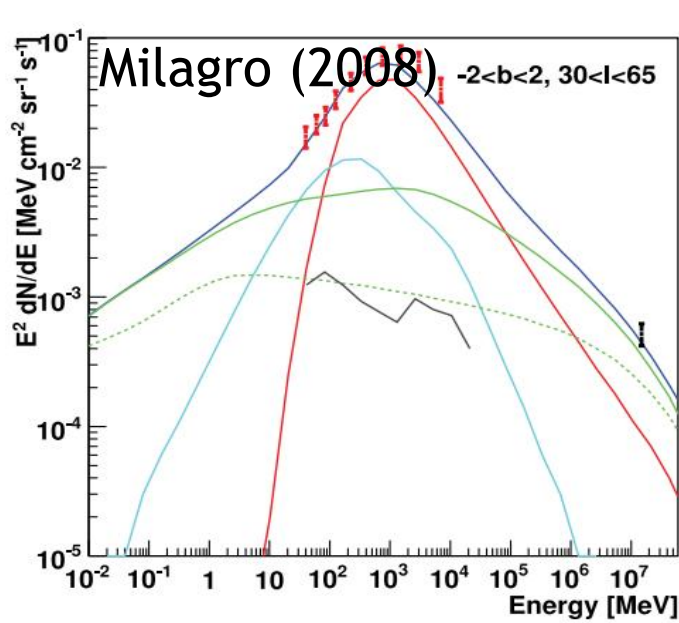


Fermi

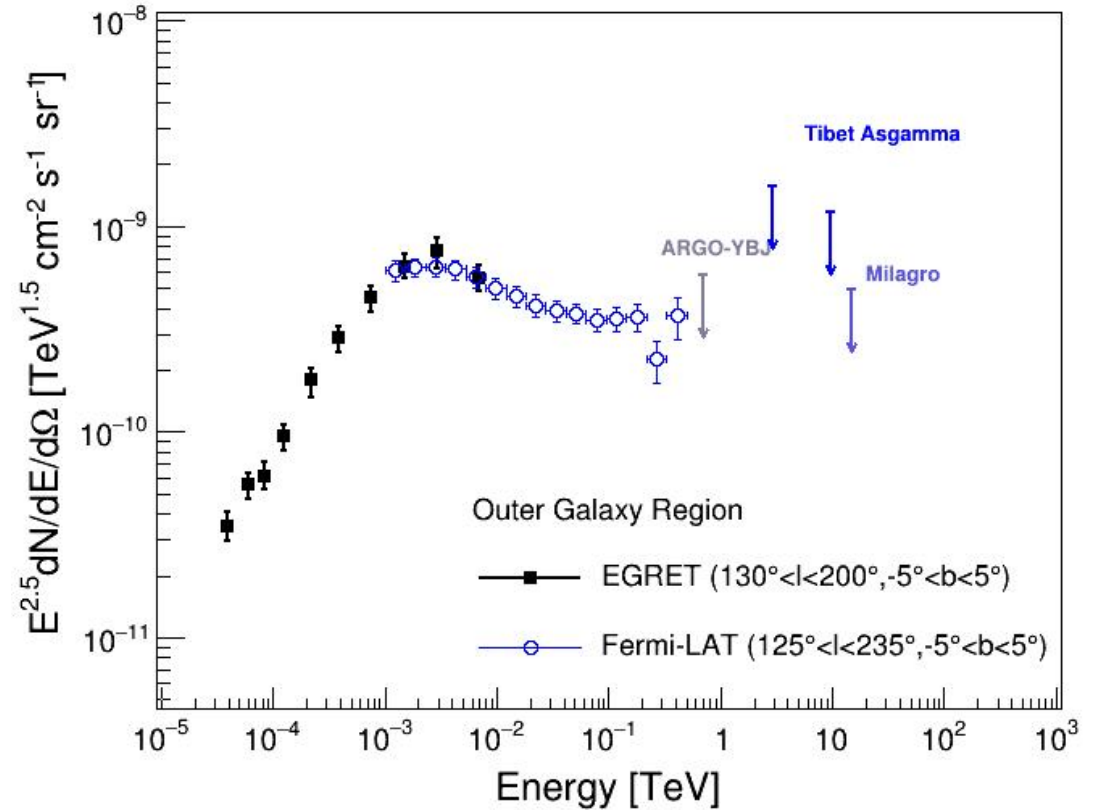
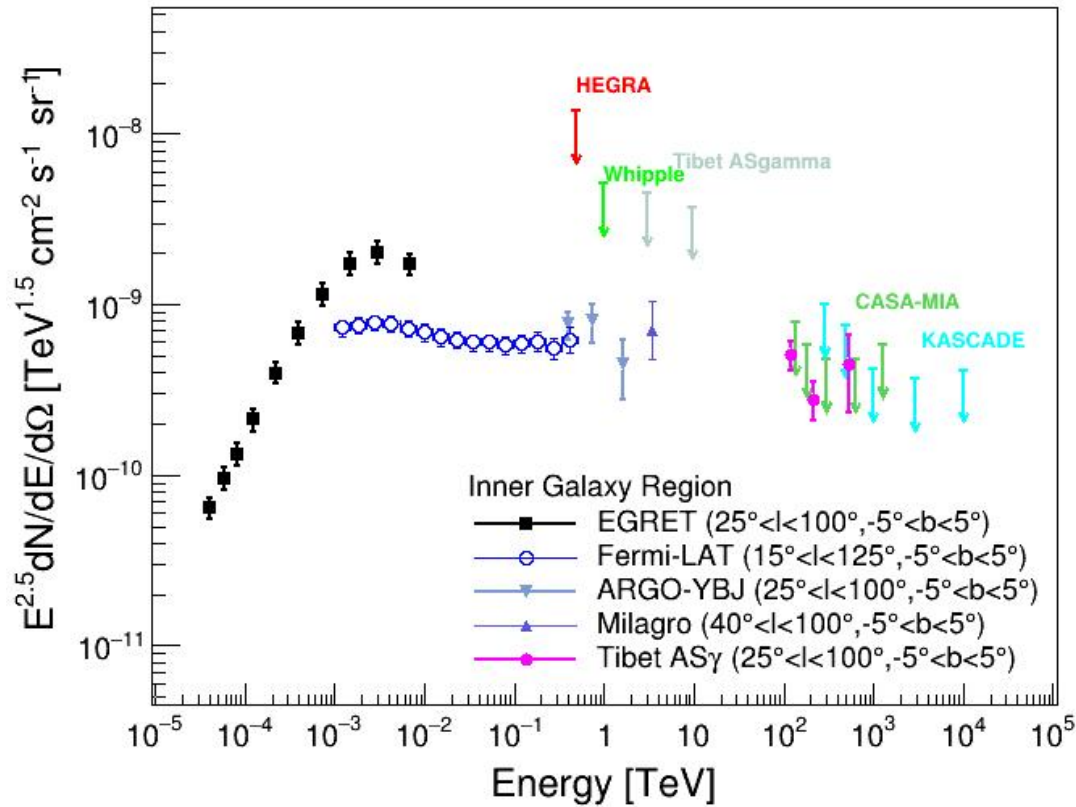




# VHE diffuse measurement on ground (>TeV)



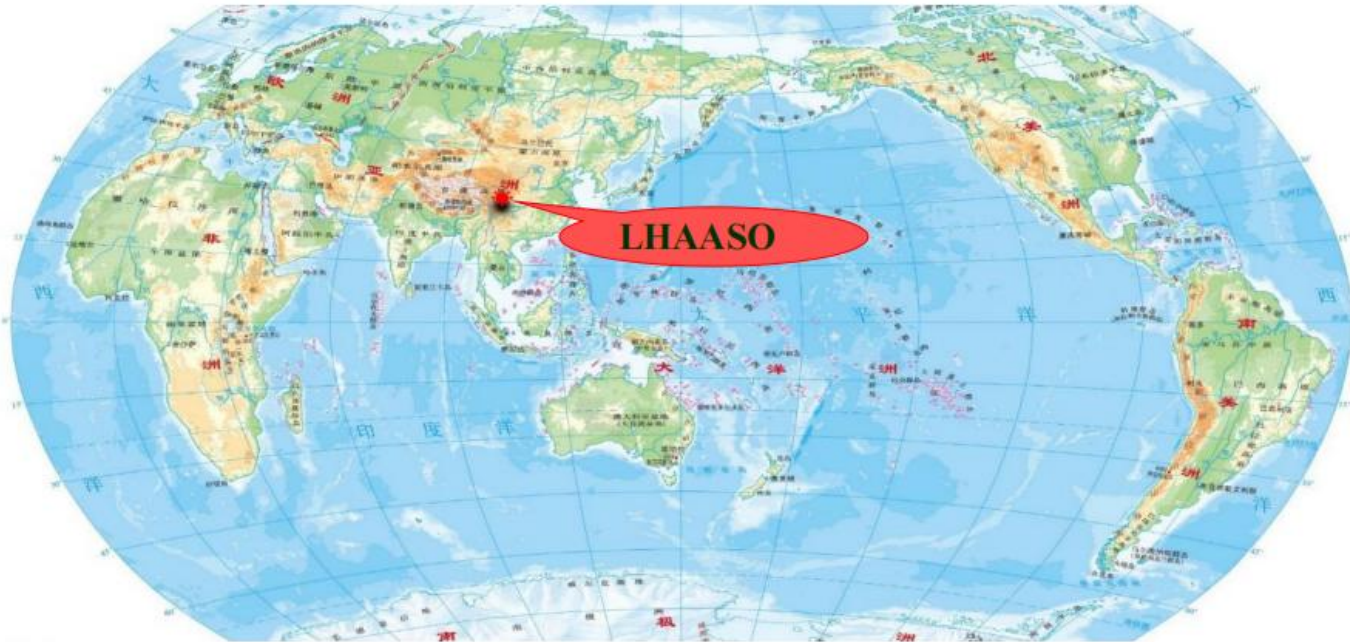
# Wide-band diffuse emission measurements



Above TeV, the energy and sky coverage is limited, especially in the outer Galactic plane region where only upper limits were given



# Large High Altitude Air Shower Observatory——LHAASO

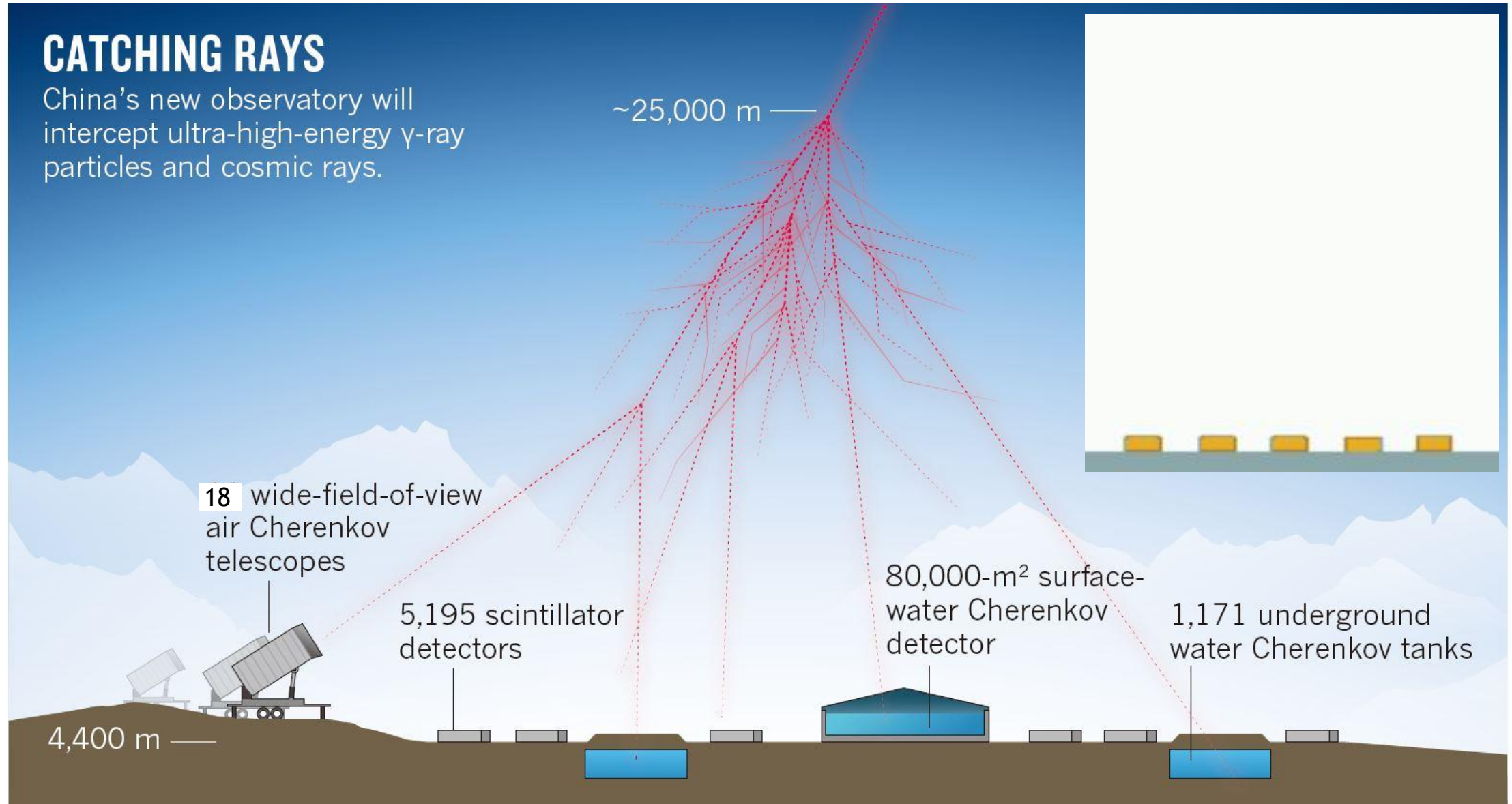


- Haizi mountain, Sichuan, China, 4410 m above the sea level
- LHAASO uses hybrid detector arrays: the square kilometer array (KM2A), the water Cherenkov detector array (WCDA), and the wide field-of-view Cherenkov telescope array (WFCTA)
- Full operation since July 2021

# Air shower detection of cosmic rays

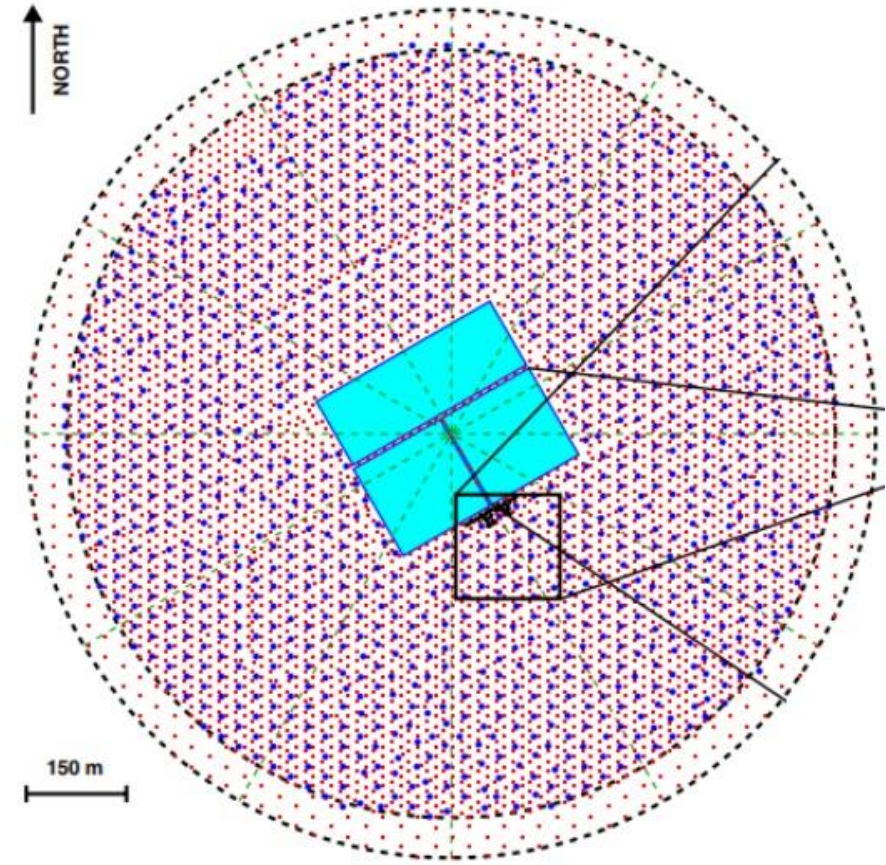
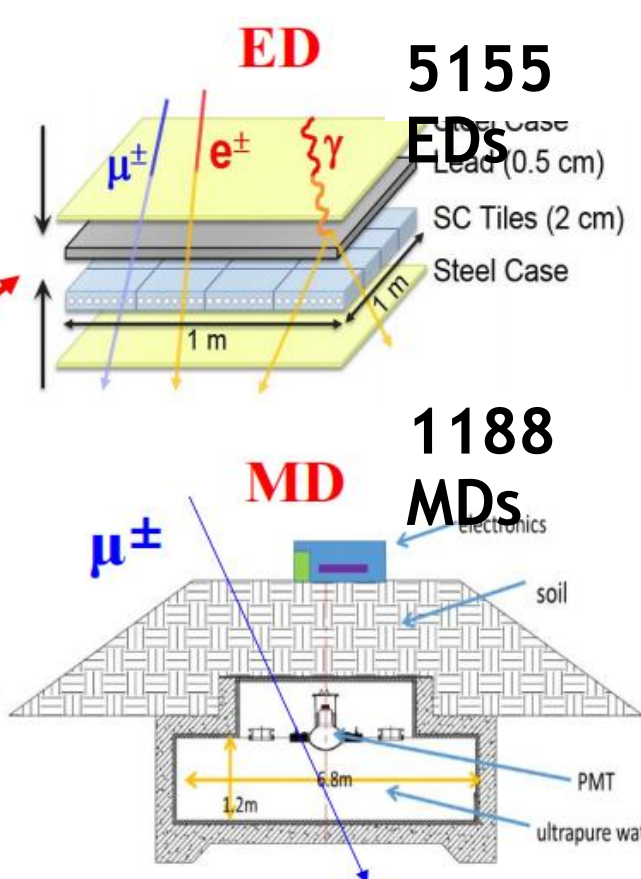
## CATCHING RAYS

China's new observatory will intercept ultra-high-energy  $\gamma$ -ray particles and cosmic rays.





# KM2A: Square Kilometer Array



- 1.3 km<sup>2</sup> area covered by 5155 electromagnetic detectors, used for energy and direction reconstruction
- 1188 muon detectors used for gamma/hadron distinguish
- Energy coverage: 10 TeV - 100 PeV



# WCDA: Water Cherenkov Detector Array



- 78000 m<sup>2</sup> water tank to detect Cherenkov light produced by air shower particles in water
- Energy coverage: 0.3 TeV - PeV

# WFCTA: Wide Field Cherenkov Telescope Array

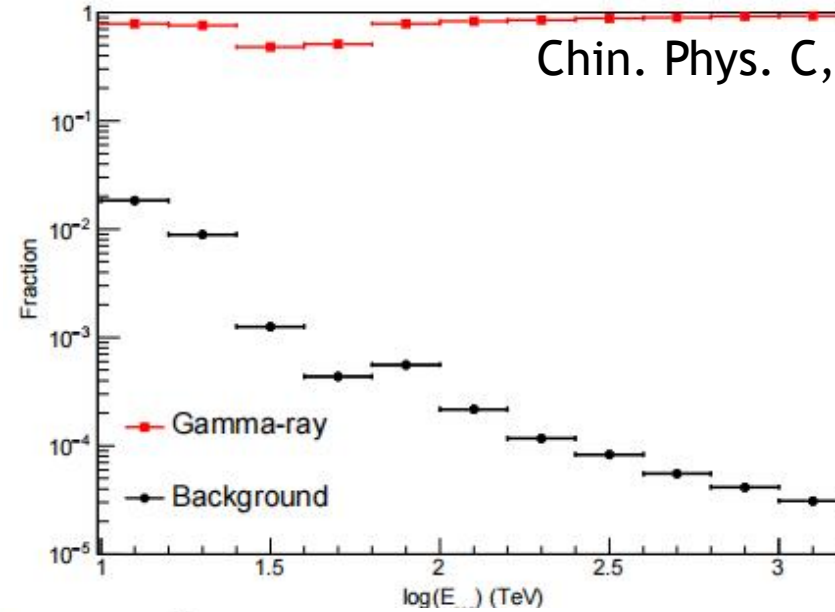
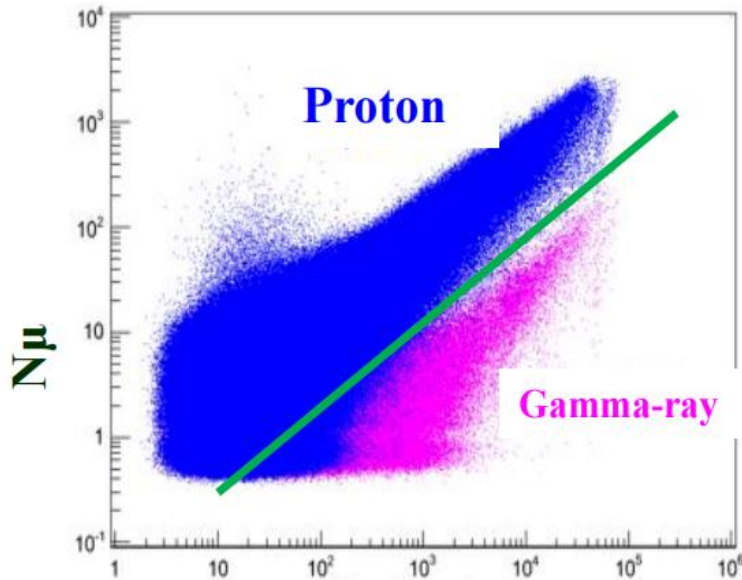


- 18 WFCTA used to distinguish particles with different mass, each one has an area of  $4.7 \text{ m}^2$  each and covers a square sky with area  $16^\circ \times 16^\circ$
- Energy coverage: 10 TeV - 100 PeV



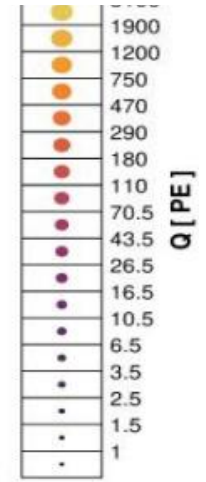
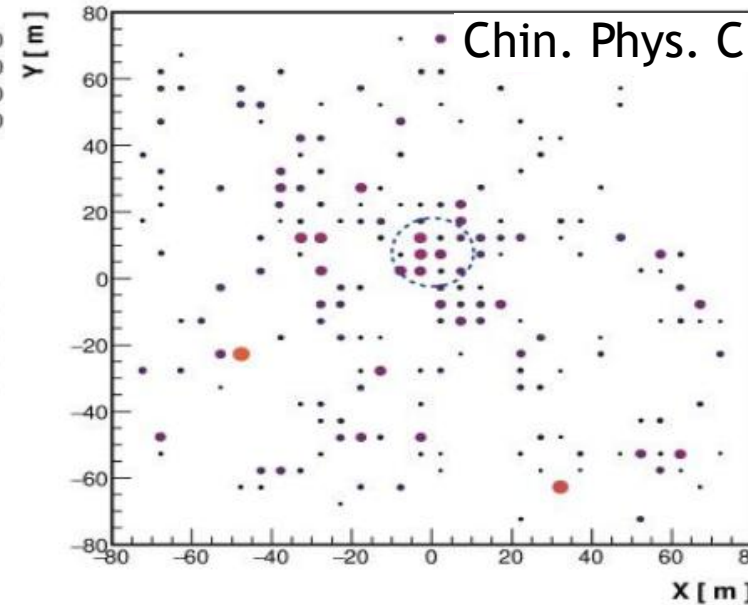
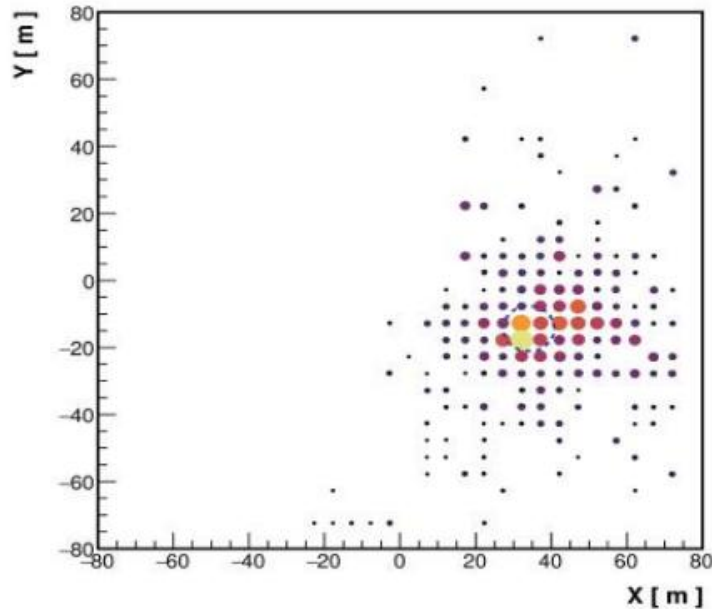
# Gamma-CR discrimination

KM2A



Chin. Phys. C, 45, 025002 (2021)

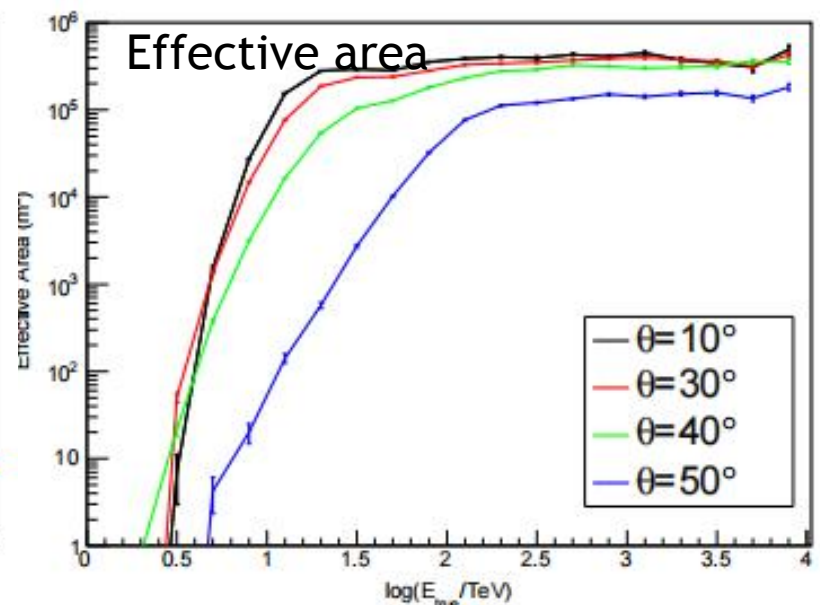
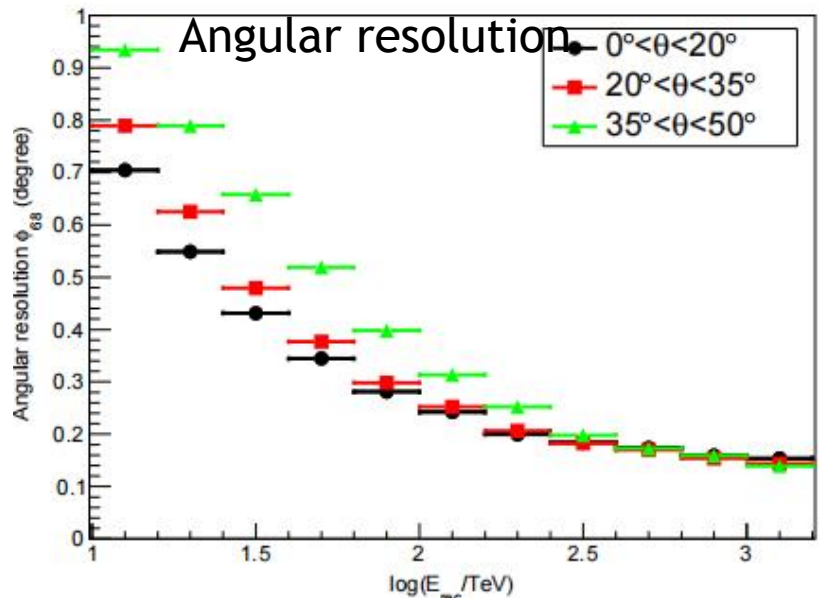
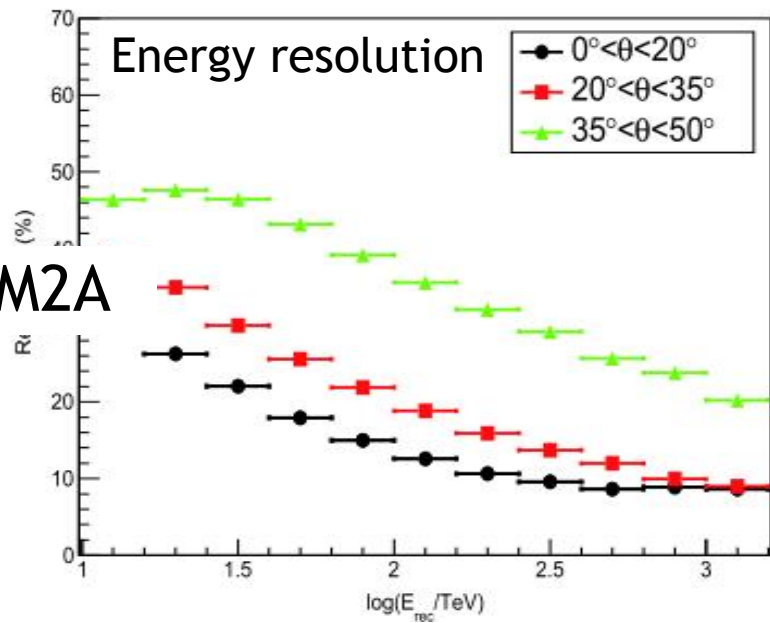
WCDA



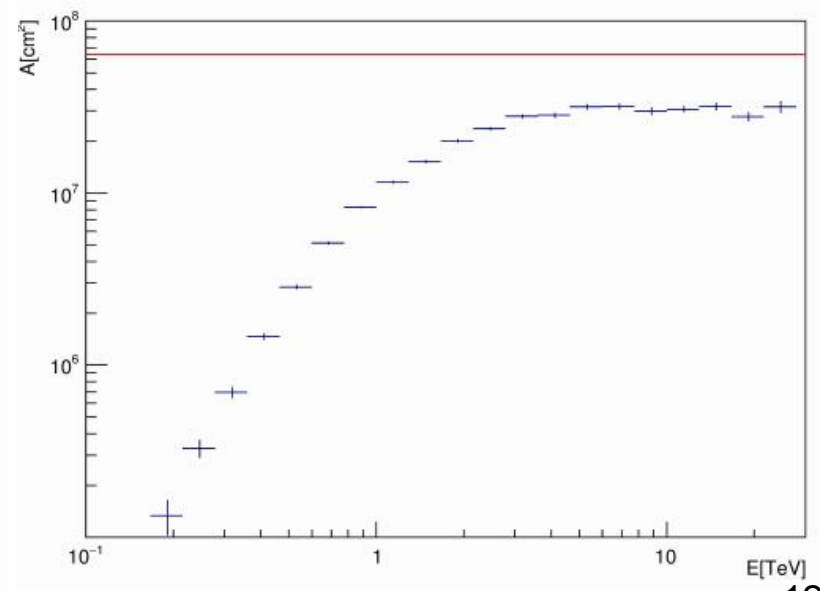
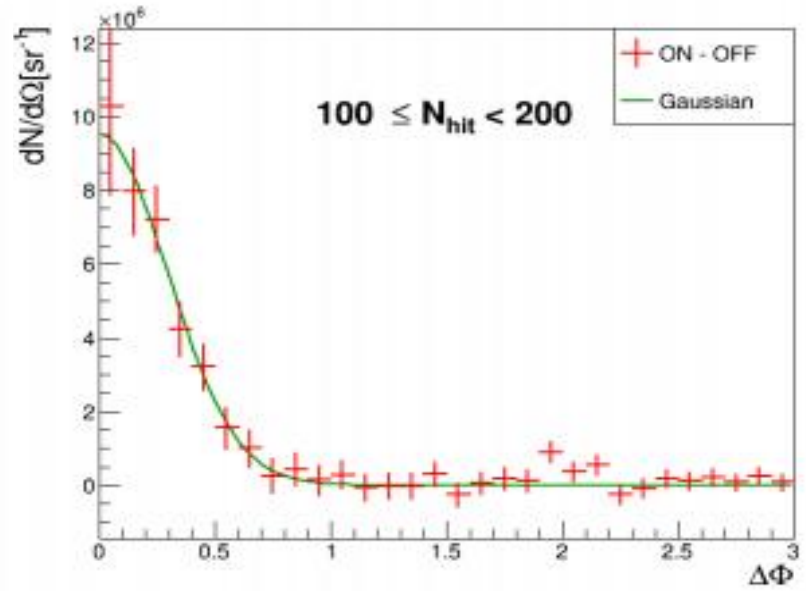
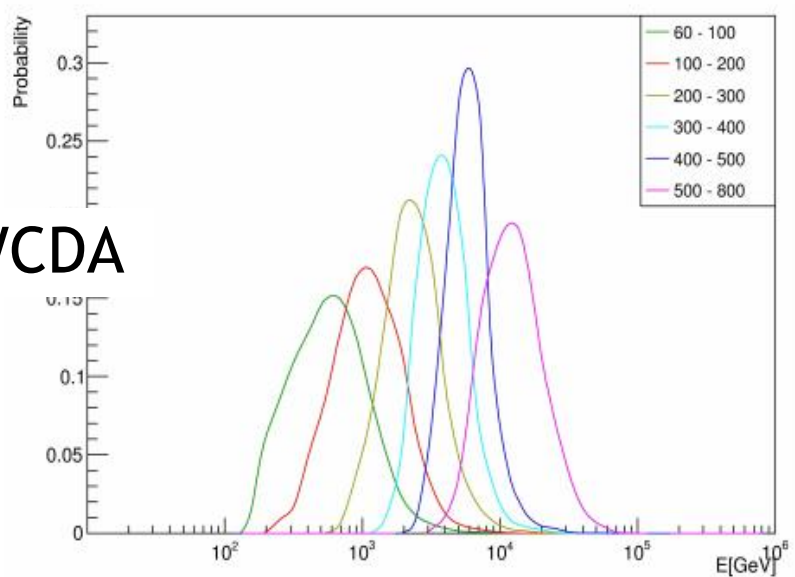
Chin. Phys. C, 45, 085002 (2021)

# Gamma-ray performance

KM2A

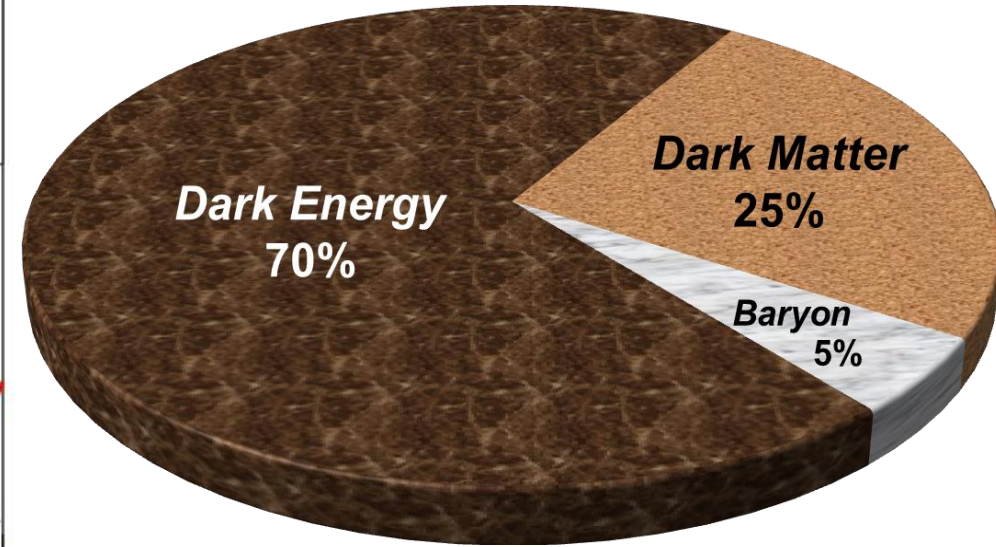
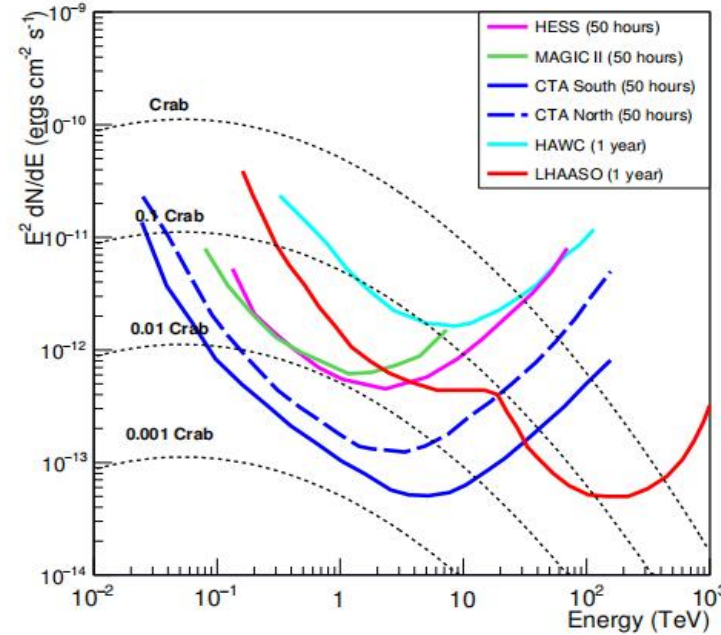
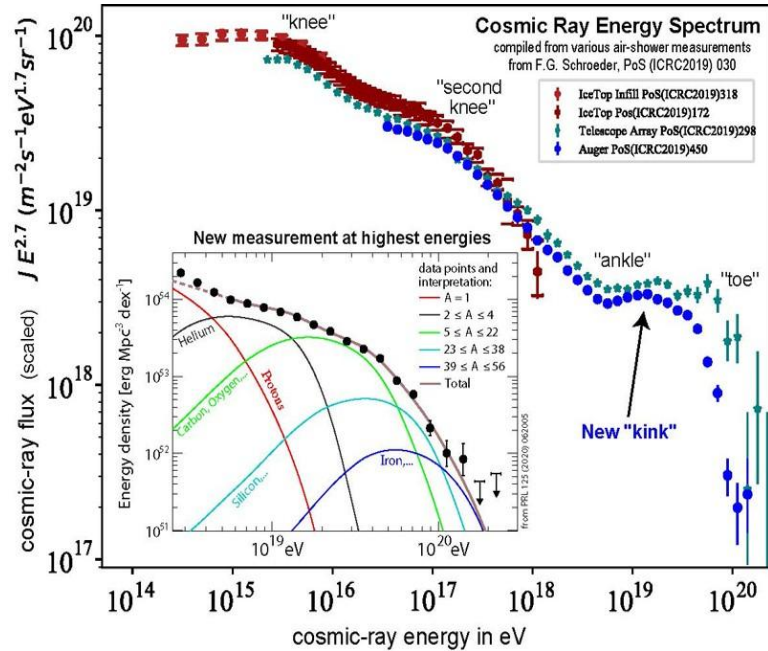


WCDA





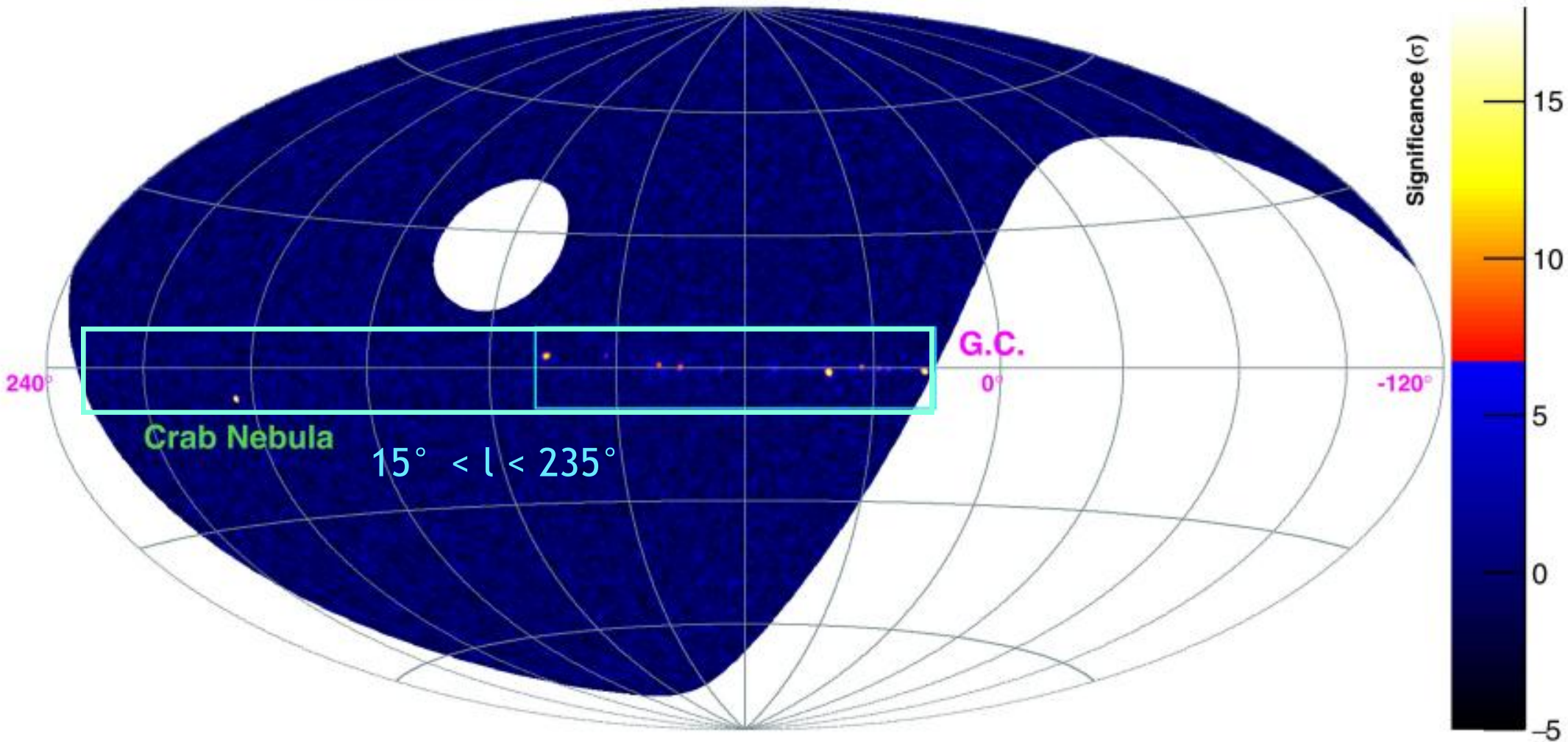
# Objectives of LHAASO



- Probe the origin of CRs, via precise measurements of spectra and anisotropies
- Survey the ultra-high-energy gamma-ray sky with unprecedented sensitivity
- Search for new physics

# LHAASO sky coverage

LHAASO Sky @ >100 TeV

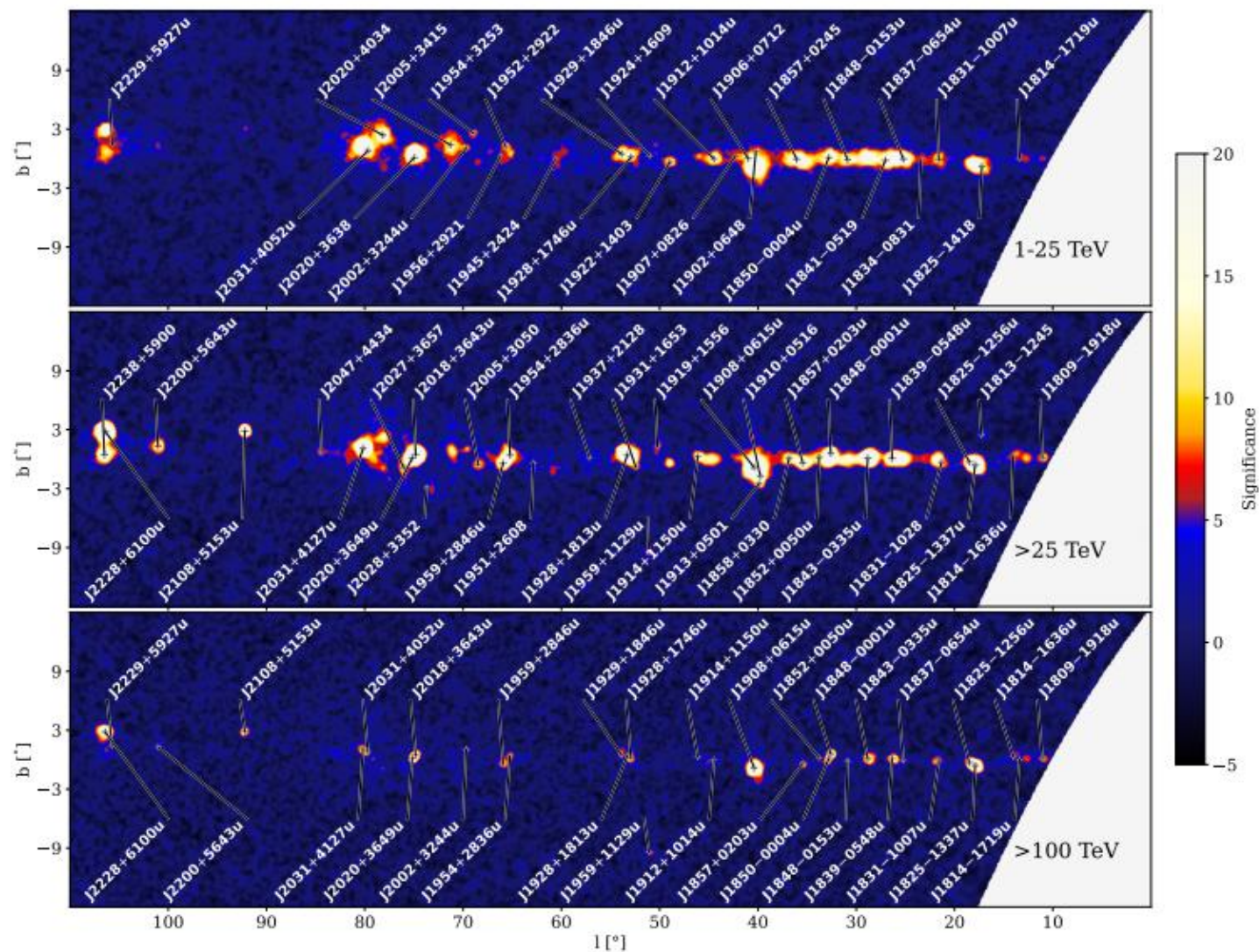




# Resolved source masks

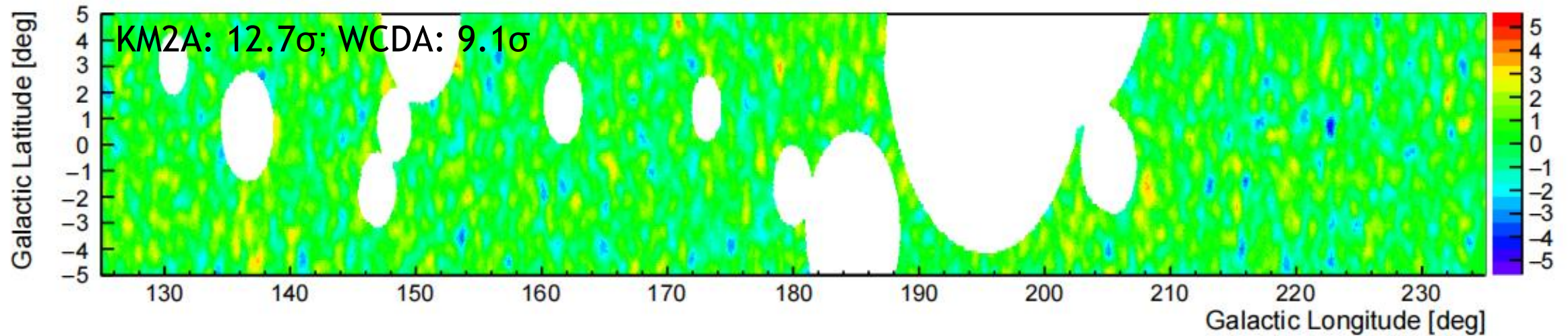
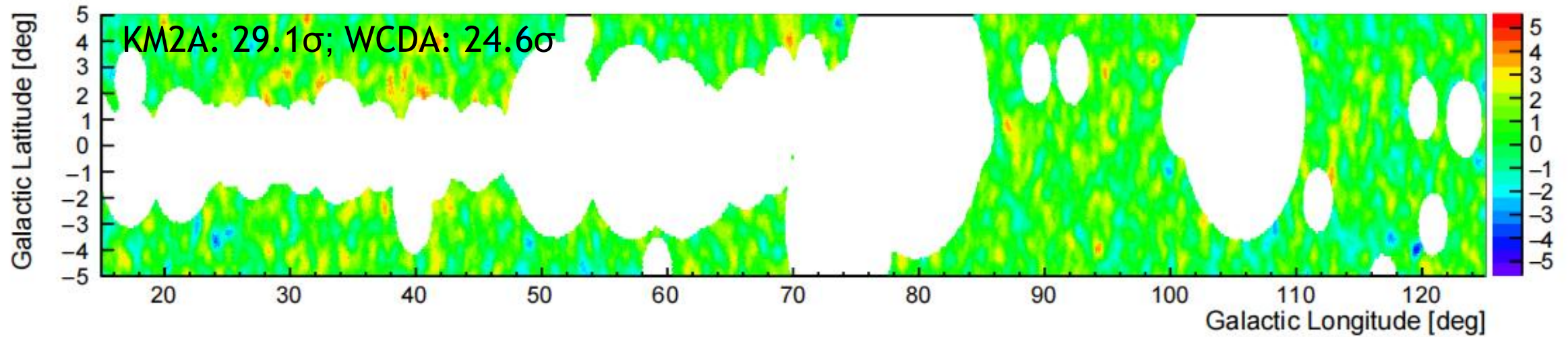
$$R_{\text{mask}} = n \cdot \sqrt{\sigma_{\text{psf}}^2 + \sigma_{\text{ext}}^2},$$

- Assumption: source morphology is Gaussian
- $n=2.5$  is chosen
- Source catalogs: LHAASO catalog + TeVCat
- For overlapping sources, LHAASO parameters are used



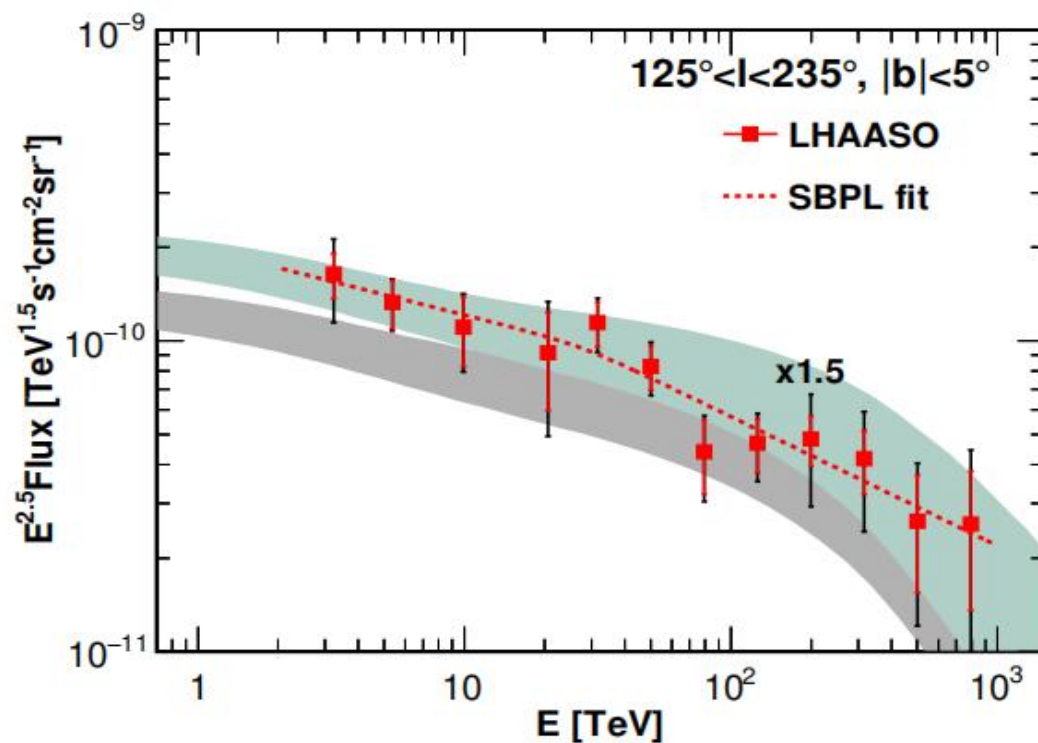
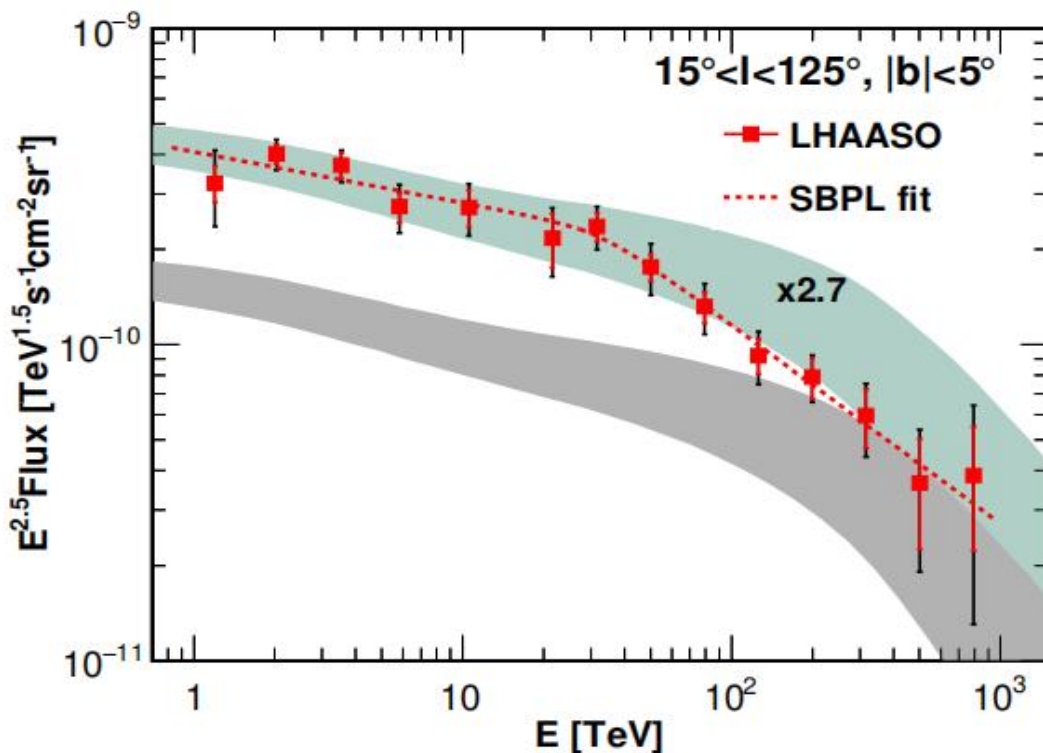


# LHAASO diffuse results





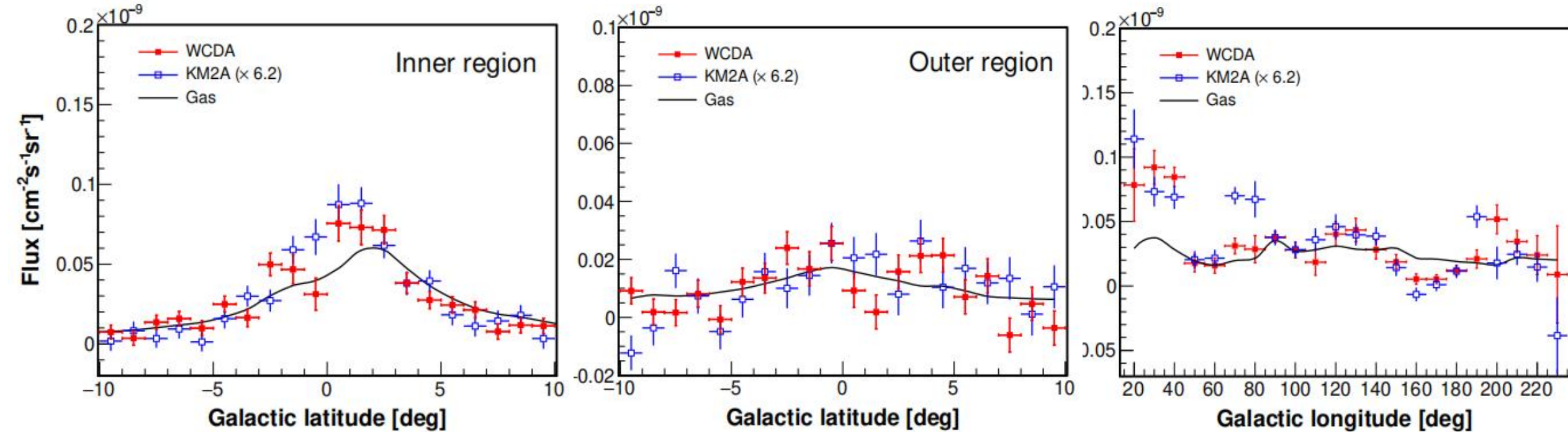
# LHAASO diffuse results



Region	$\phi_0$ at 10 TeV ( $10^{-13} \text{ TeV}^{-1} \text{ cm}^{-2} \text{ s}^{-1} \text{ sr}^{-1}$ )	$\alpha$	$\beta$	$E_{\text{br}}$ (TeV)
$15^\circ < l < 125^\circ$ (inner)	$8.88 \pm 0.53_{\text{stat}}$	$-2.66 \pm 0.05_{\text{stat}}$	$-3.13 \pm 0.08_{\text{stat}}$	$32.84 \pm 11.16_{\text{stat}}$
$125^\circ < l < 235^\circ$ (outer)	$3.84 \pm 0.37_{\text{stat}}$	$-2.72 \pm 0.10_{\text{stat}}$	$-2.92 \pm 0.10_{\text{stat}}$	$27.86 \pm 22.49_{\text{stat}}$

- LHAASO measures diffuse emission from 1 TeV to 1 PeV with high significance, and gives the first detection from the outer Galactic plane
- A spectral break around 30 TeV is revealed in the inner Galactic plane

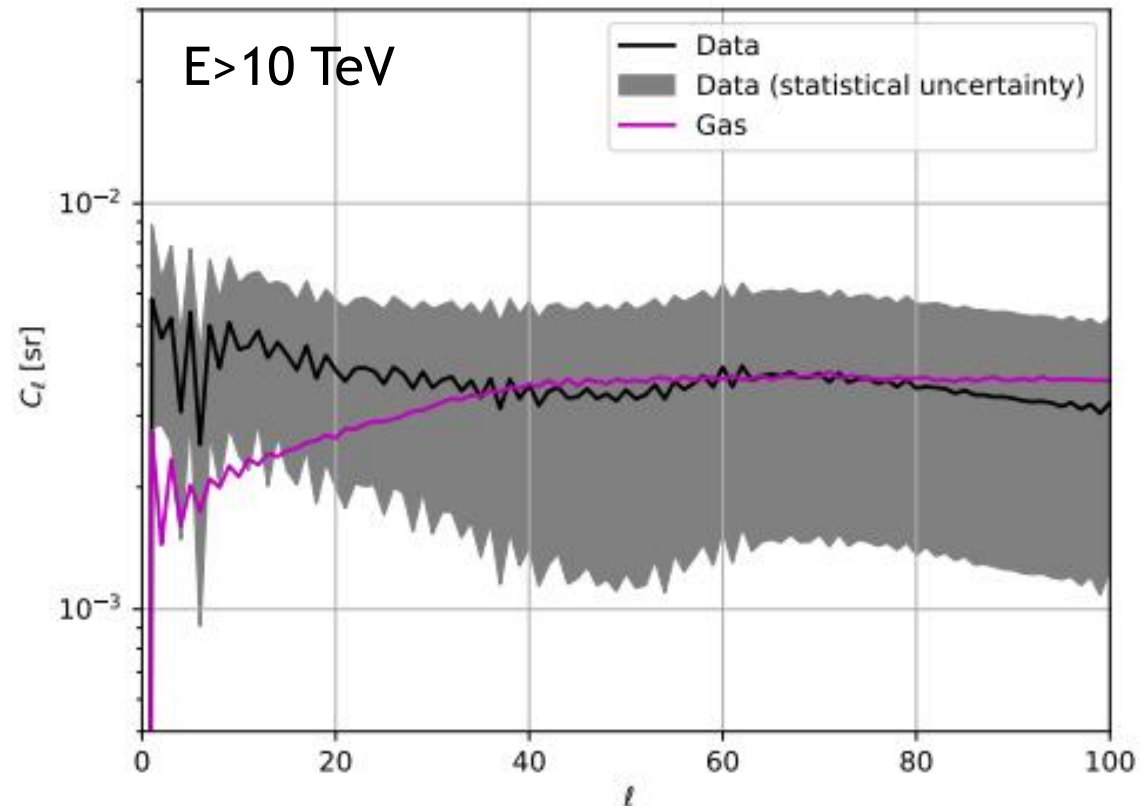
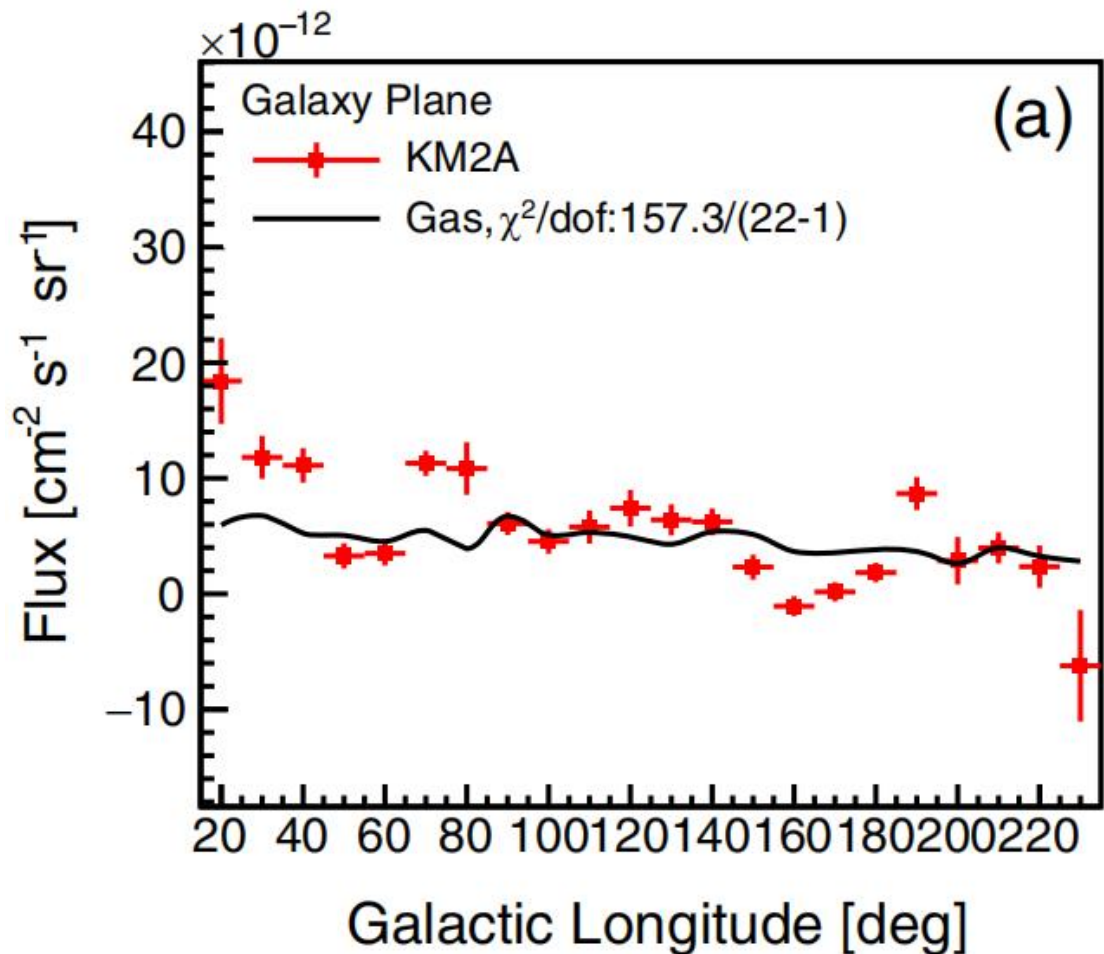
# Longitude and latitude profiles



Roughly consistent with gas distributions for  $b$ , but show **significant** deviation for  $l$



# Spatial distribution



Difference between data and gas is also shown in the angular spectra at low- $l$

# Possible spatial variation of spectra

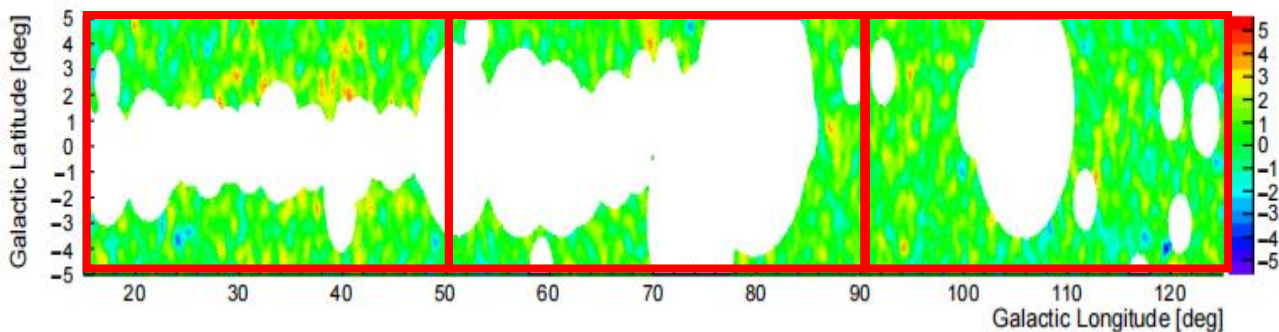
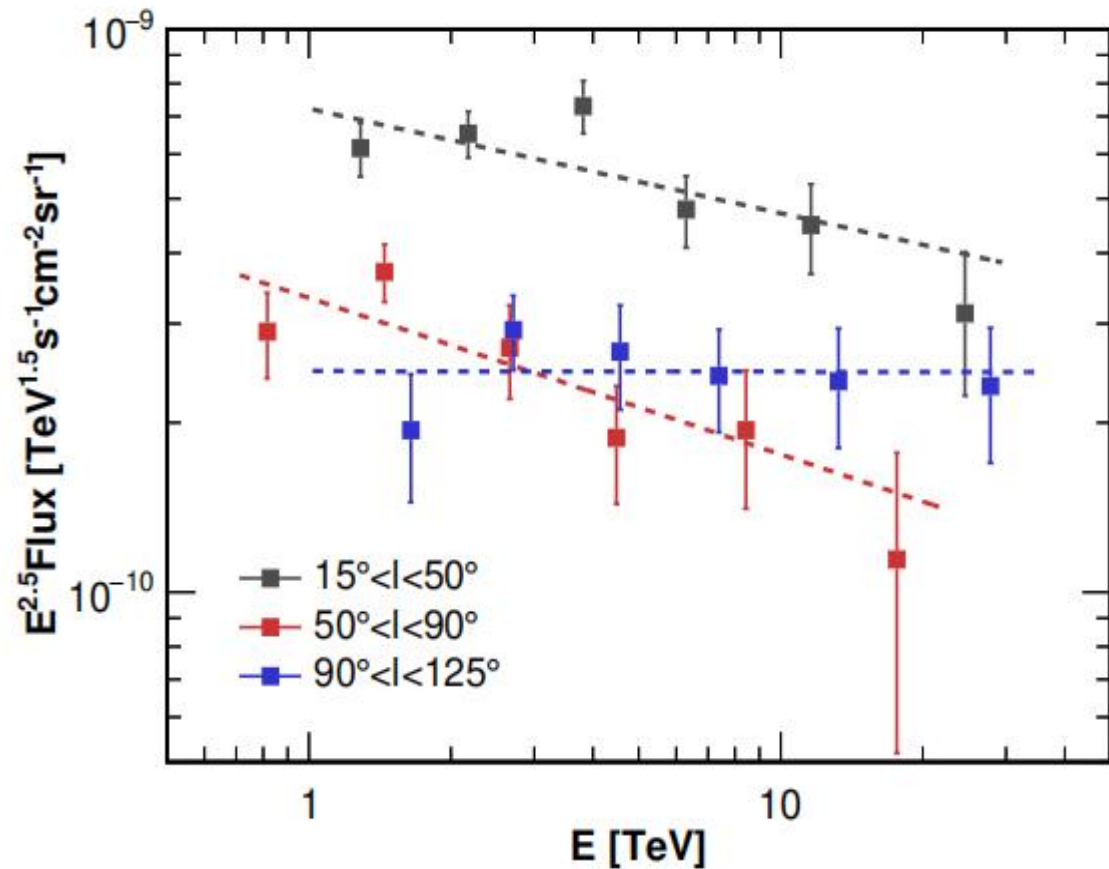


TABLE II. Power-law fitting results of the LHAASO-WCDA diffuse emission.

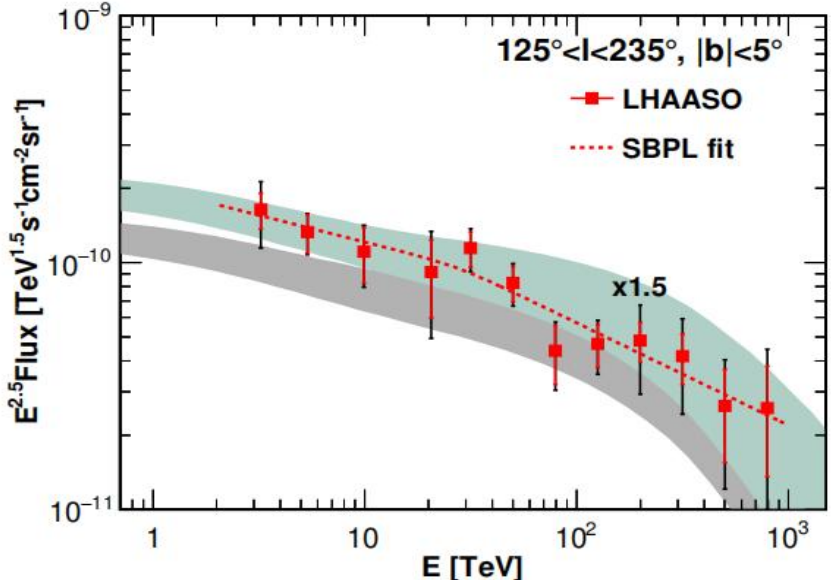
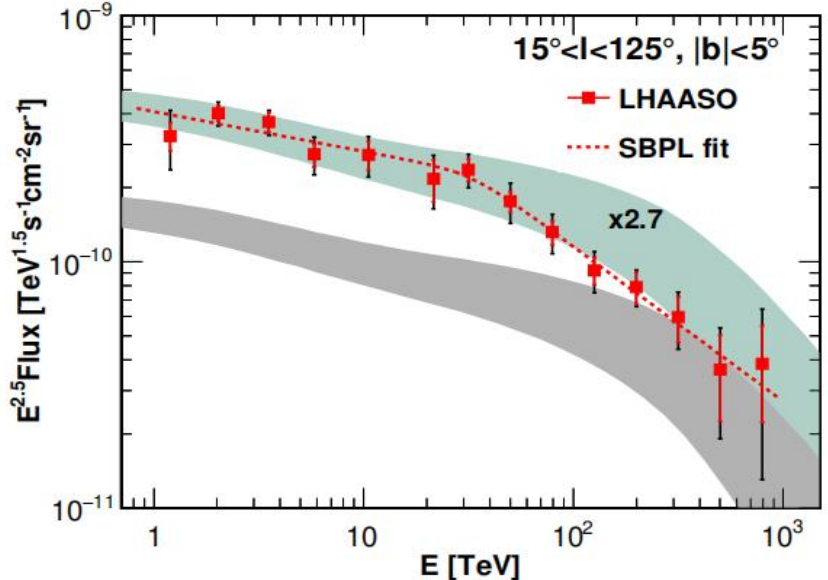
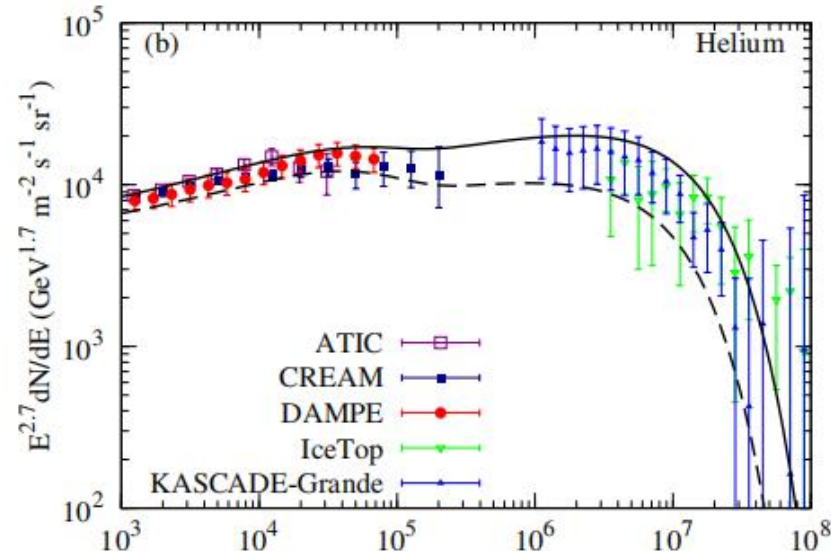
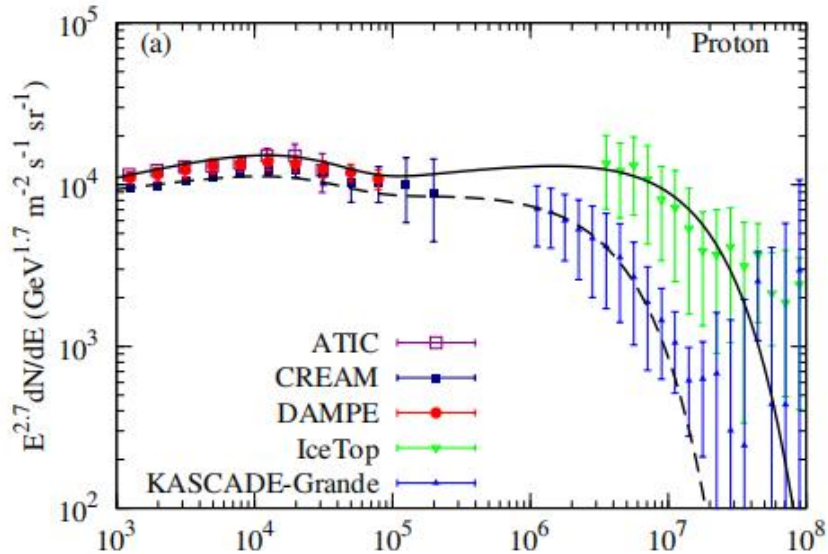
Region	$\phi_0$ at 10 TeV ( $10^{-13} \text{ TeV}^{-1} \text{ cm}^{-2} \text{ s}^{-1} \text{ sr}^{-1}$ )	$\alpha$
$15^\circ < l < 125^\circ$ (inner)	$8.50 \pm 0.58_{\text{stat}}$	$-2.67 \pm 0.05_{\text{stat}}$
$125^\circ < l < 235^\circ$ (outer)	$3.49 \pm 0.55_{\text{stat}}$	$-2.83 \pm 0.19_{\text{stat}}$
$15^\circ < l < 50^\circ$	$14.88 \pm 1.26_{\text{stat}}$	$-2.69 \pm 0.06_{\text{stat}}$
$50^\circ < l < 90^\circ$	$5.55 \pm 0.91_{\text{stat}}$	$-2.78 \pm 0.09_{\text{stat}}$
$90^\circ < l < 125^\circ$	$7.79 \pm 0.81_{\text{stat}}$	$-2.50 \pm 0.09_{\text{stat}}$



Hints of spectral variations across the Galactic plane ( $\sim 2\sigma$ )



# Confront LHAASO data with a toy model



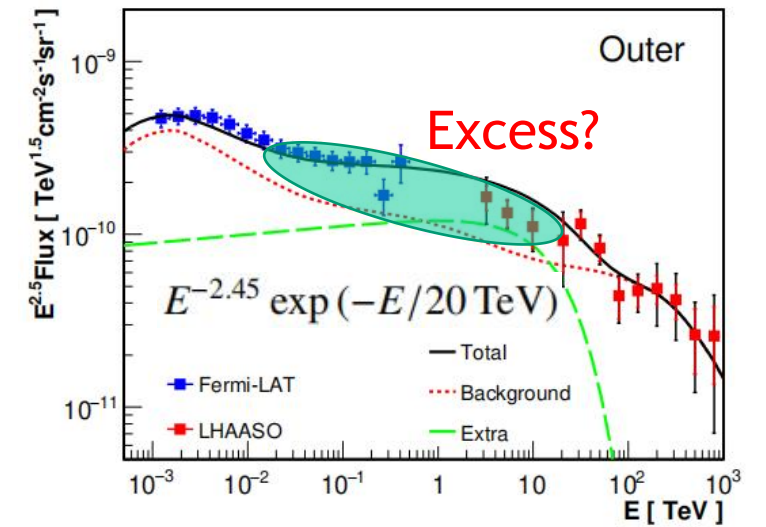
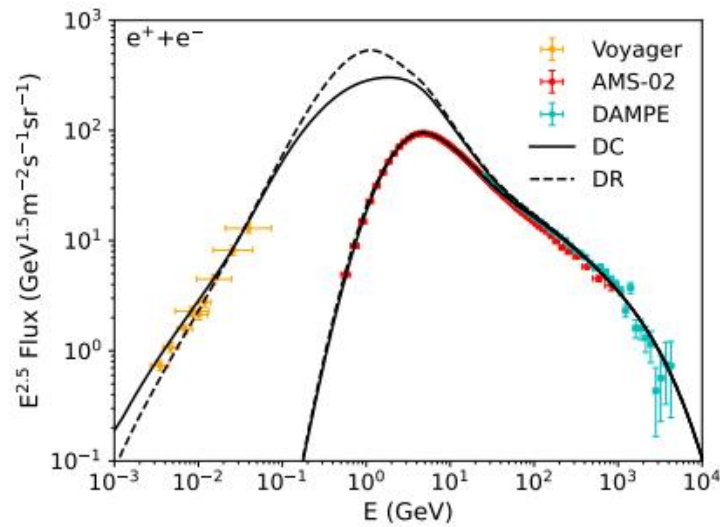
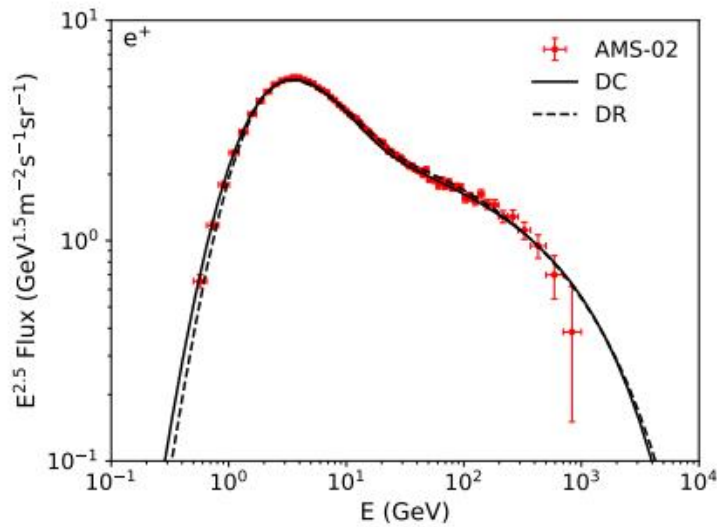
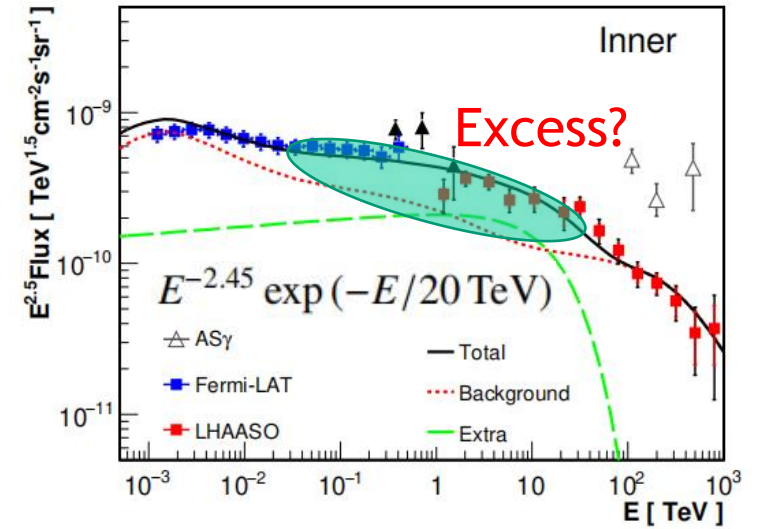
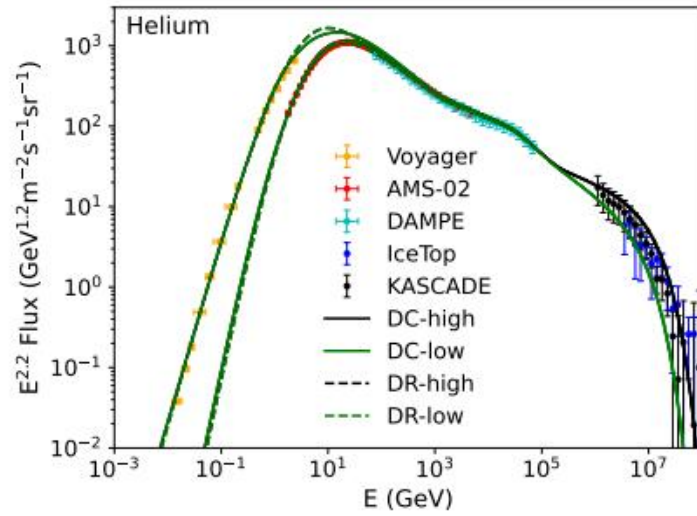
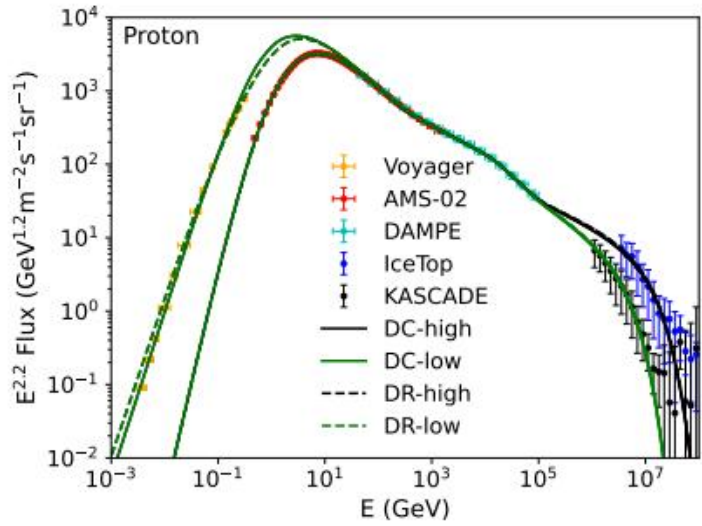
➤ Toy model prediction:  
local CR  $\times$  gas column

➤ Measured fluxes are higher by a factor of 1.5~2.7 than predictions

➤ Spectra are slightly different from the prediction

Expectation could be improved significantly with LHAASO CR measurement!

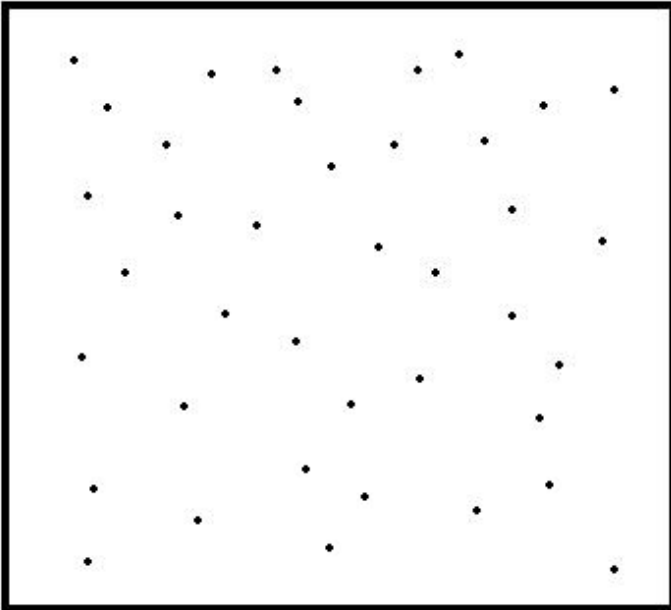
# Confront LHAASO data with a GALPROP model



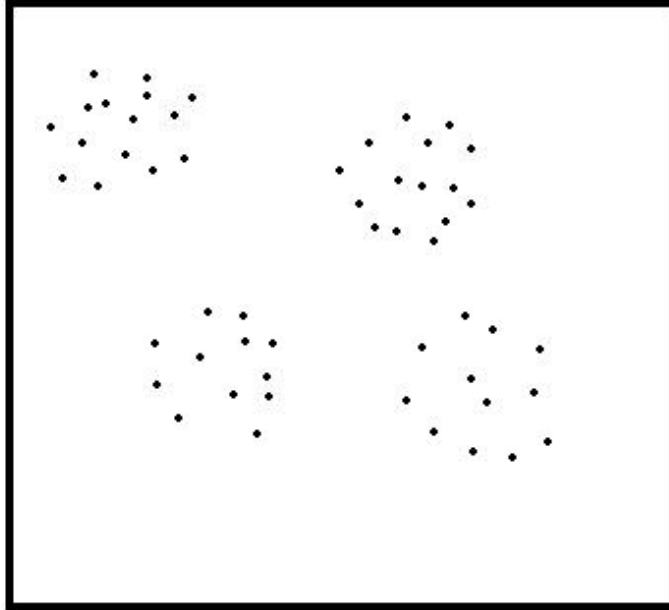


# Caveat: no distinct definition between sources and diffuse

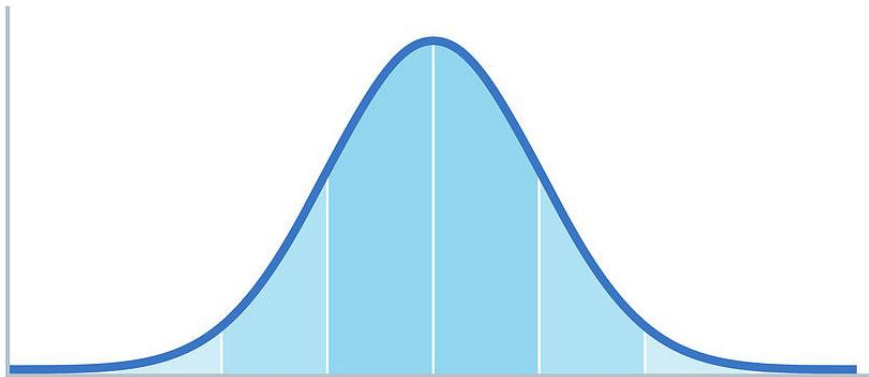
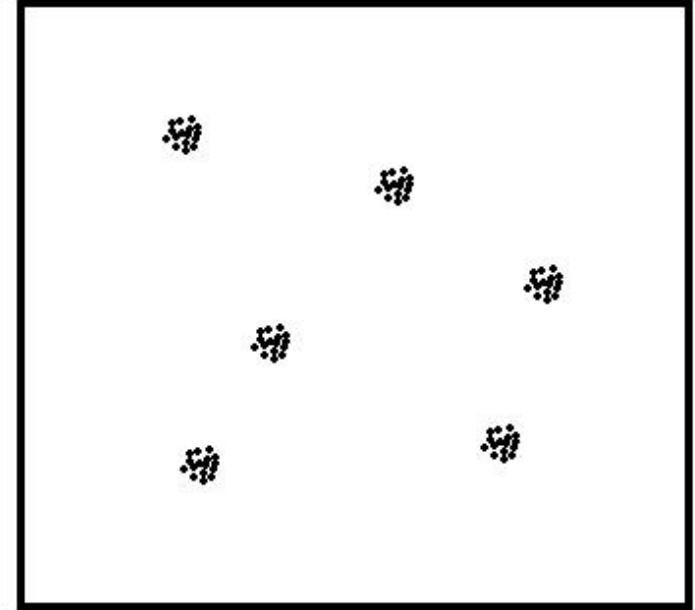
Truly diffuse  
(adequate prop.)



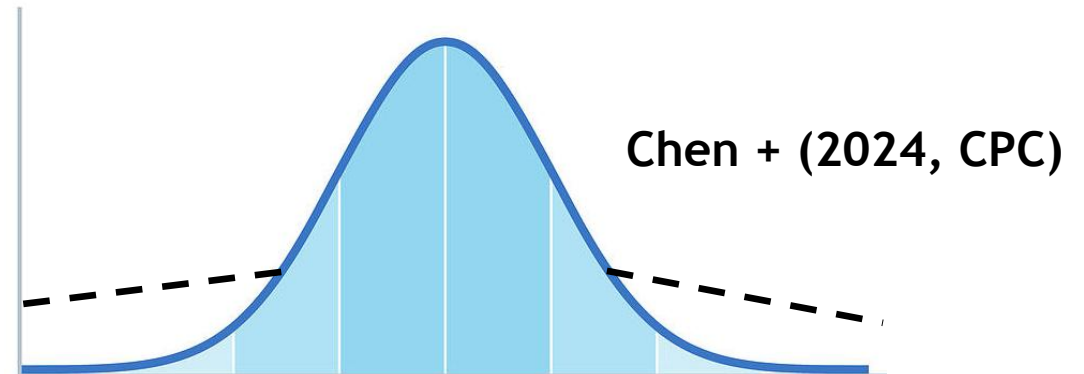
large extended source  
(non-adequate prop.)



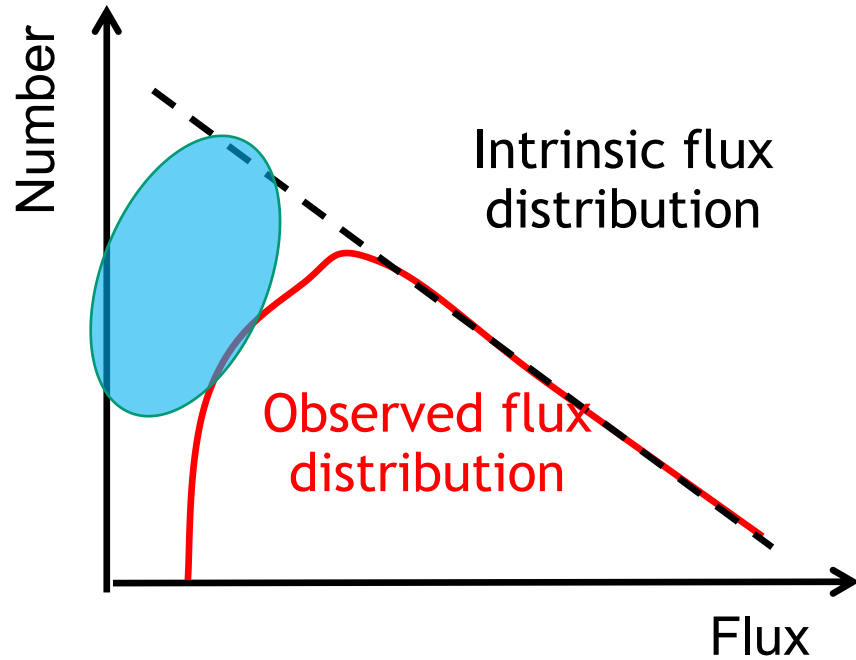
pointlike sources  
(freshly accelerated)



VS.

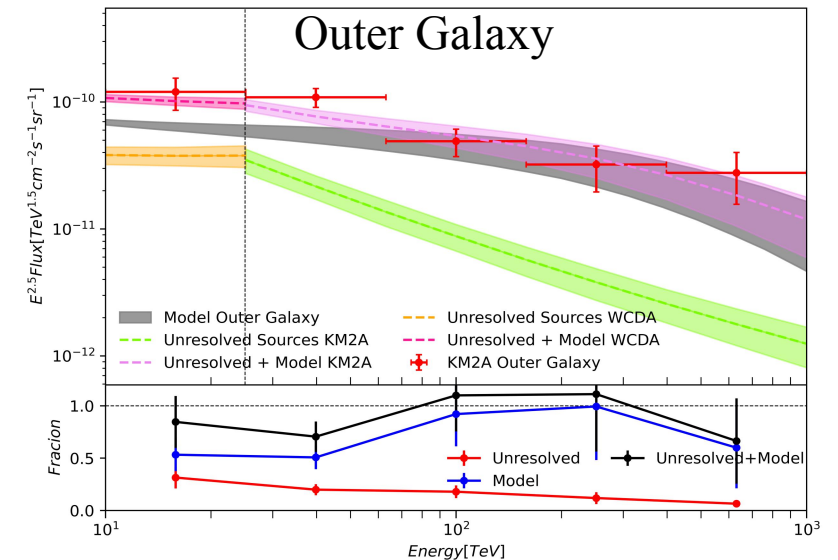
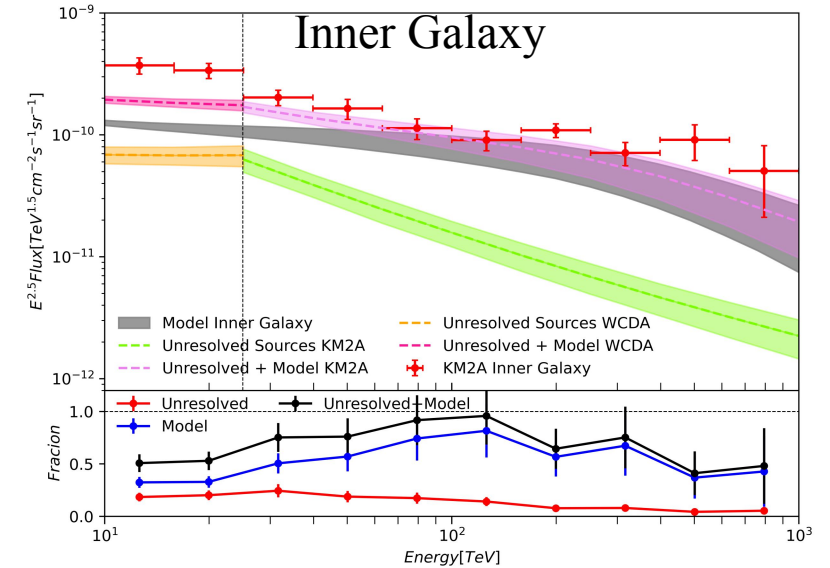


# Unresolved source contribution?



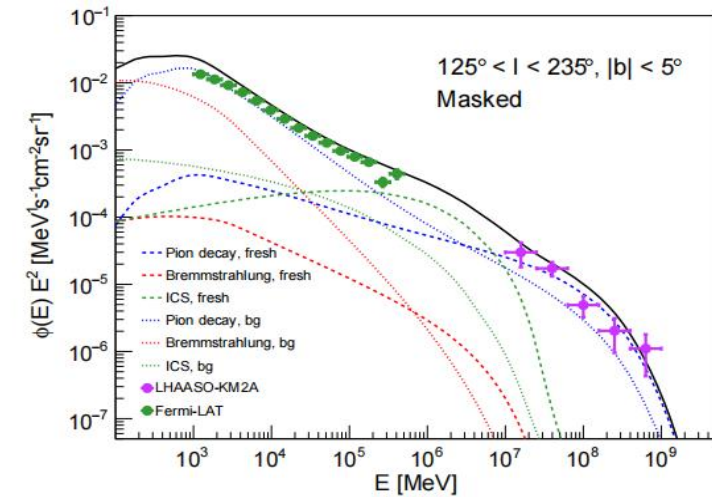
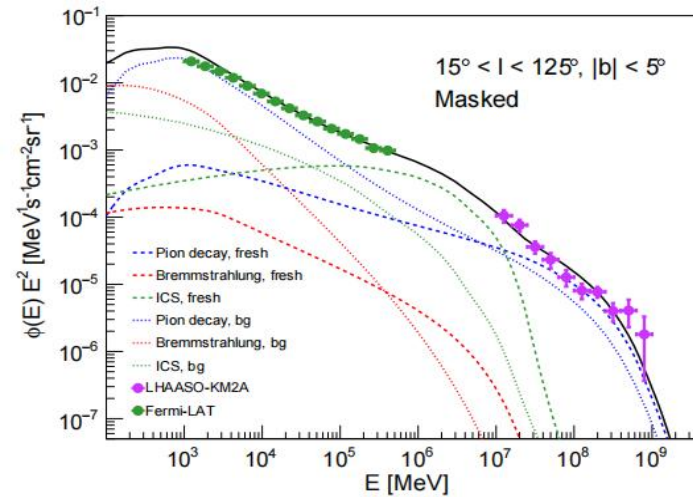
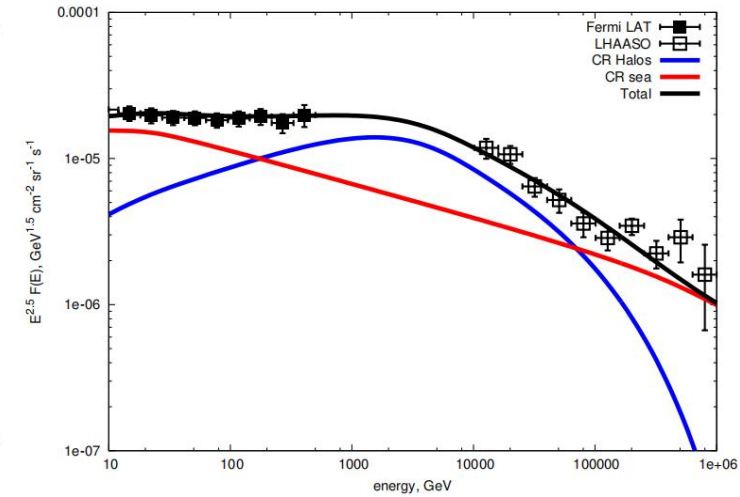
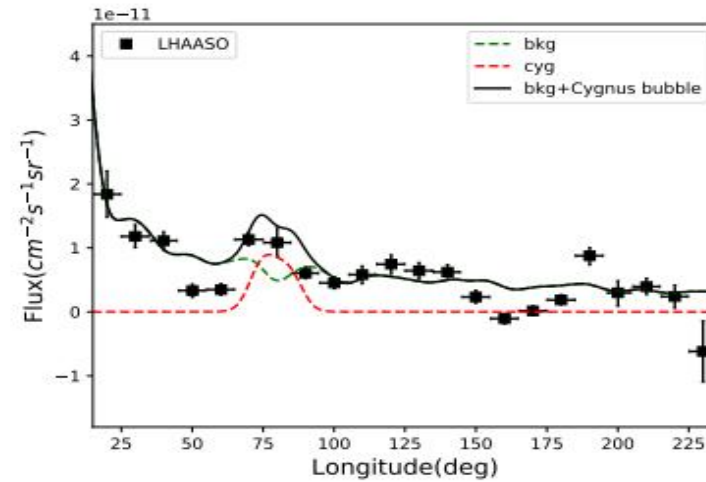
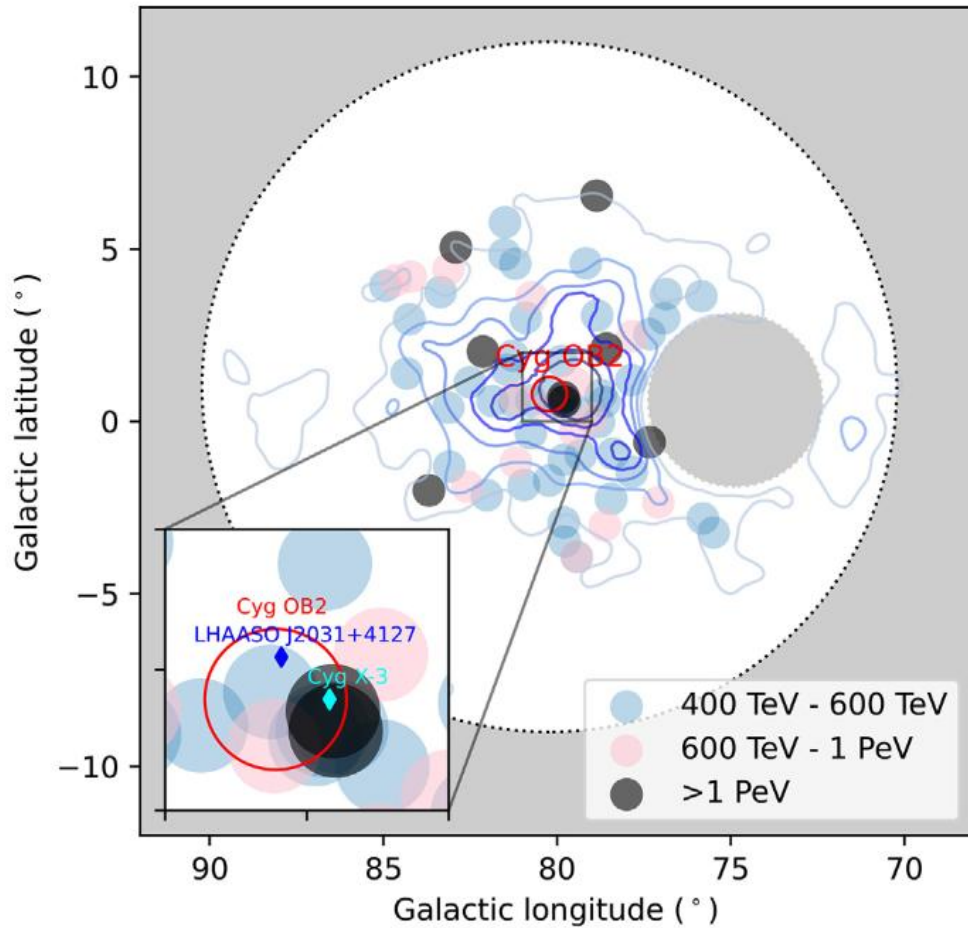
- ✓ The contribution of unresolved sources is able to describe the extra component for Outer Galaxy region, while it is insufficient for Inner Galaxy region.
- ✓ Larger extended sources were not included
- ✓ Additional contributions from unknown mechanisms

He + (2025, ApJ); Kaci + (2024, ApJ)





# Confinement and interaction around sources



Cygnus bubble: super accelerator as extended as 10 degrees (LHAASO 2024, Sci. Bull.)

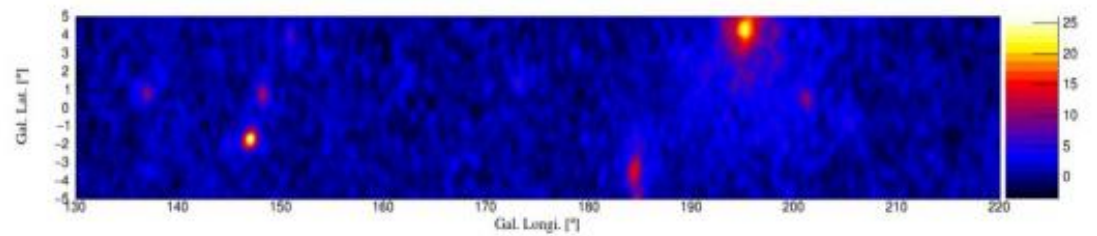
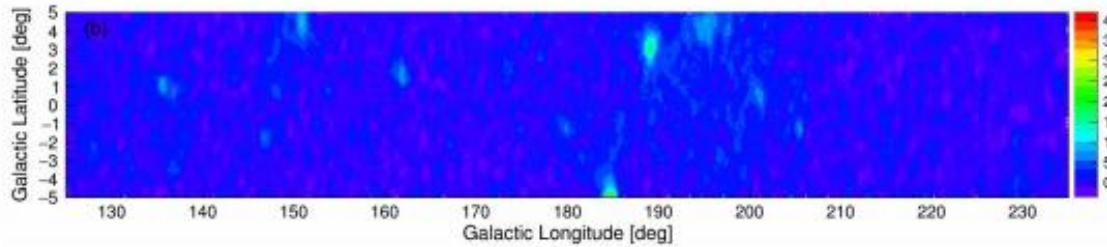
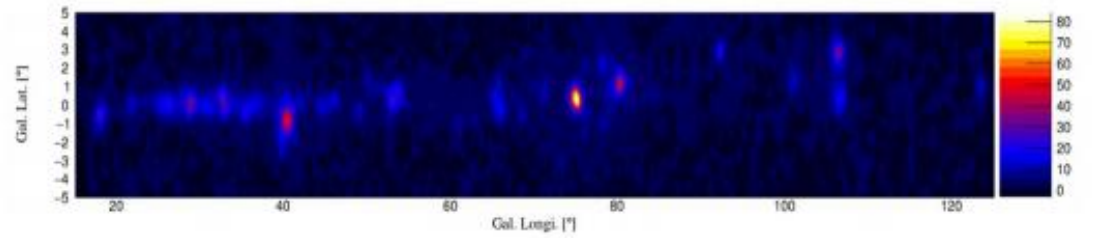
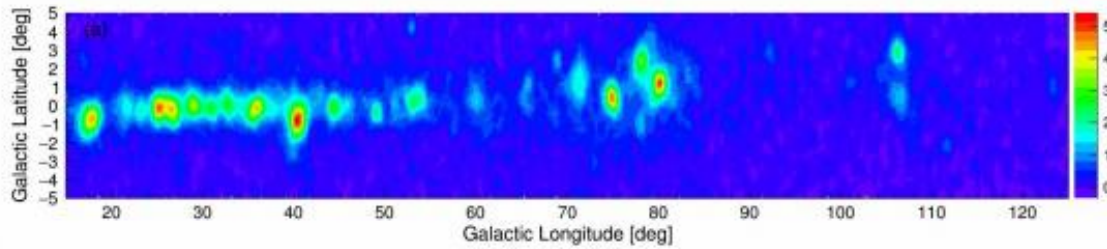
Nie + ApJ (2024); He + ApJ (2024);  
Yang & Aharonian (2024); Ambrosone + (2025)

# Other interpretations

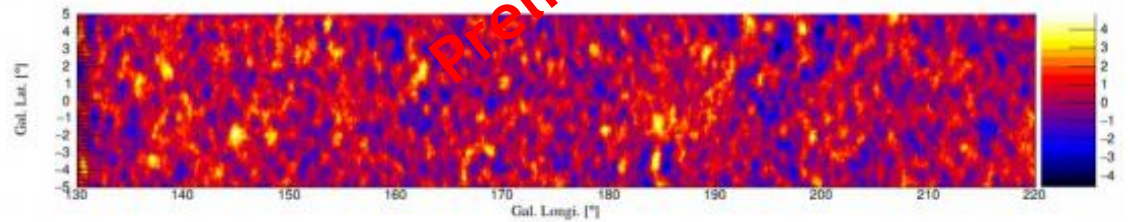
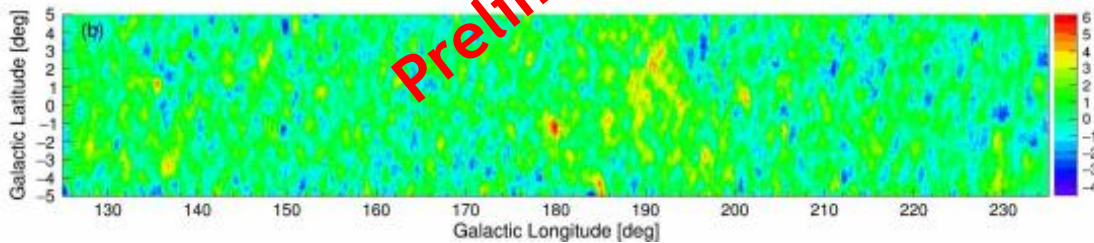
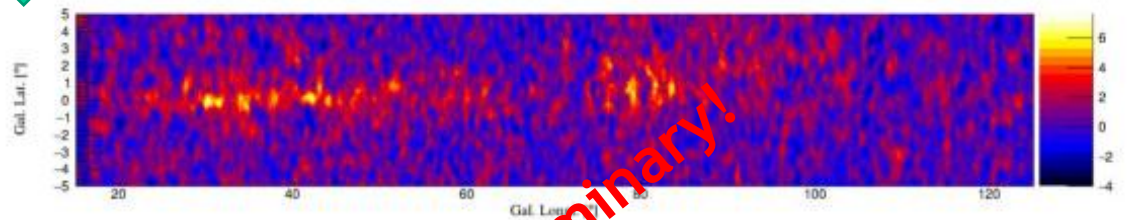
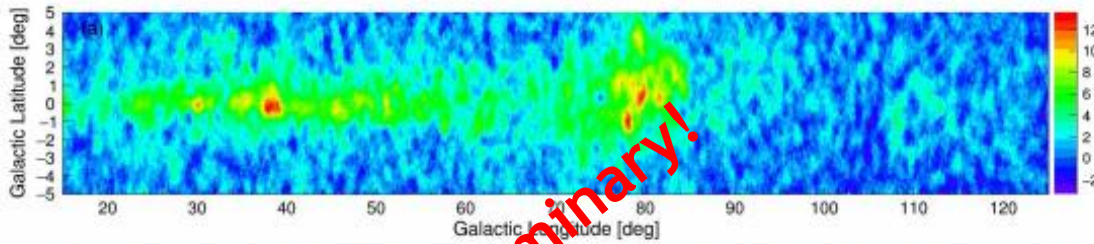
- Various types of unresolved sources: pulsar halo/PWN (Pagliaroli + 2023 Universe; Yan + 2024 Nat. Astron.; Dekker + 2024 PRD; Chen + 2024 CPC), X-ray binaries (Yue + 2024; Kuze + 2025), massive star clusters (Menchiari + 2024) ...
- Cosmic ray sea interaction with alternative propagation setup (Giacinti + 2023; Vecchiotti + 2024; De La Torre Luque + 2025)
- Time-dependent model of discrete sources (Marinos + 2024)



# Improved measurement is important



source subtraction



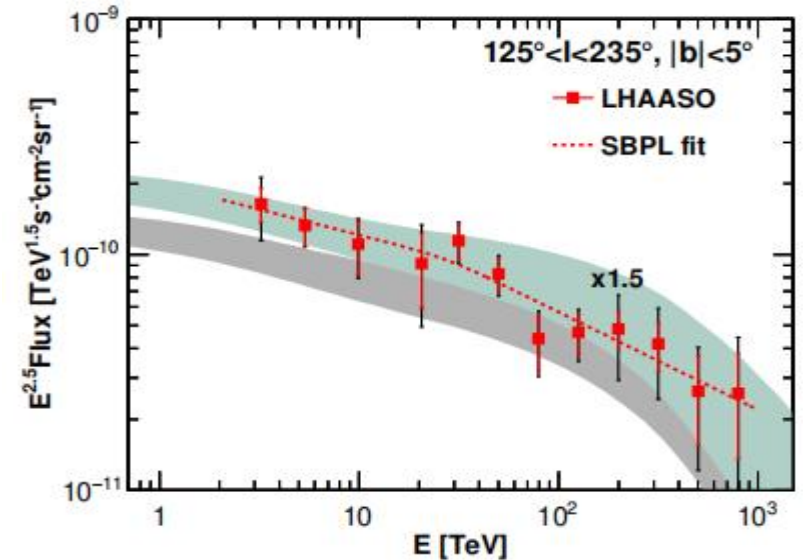
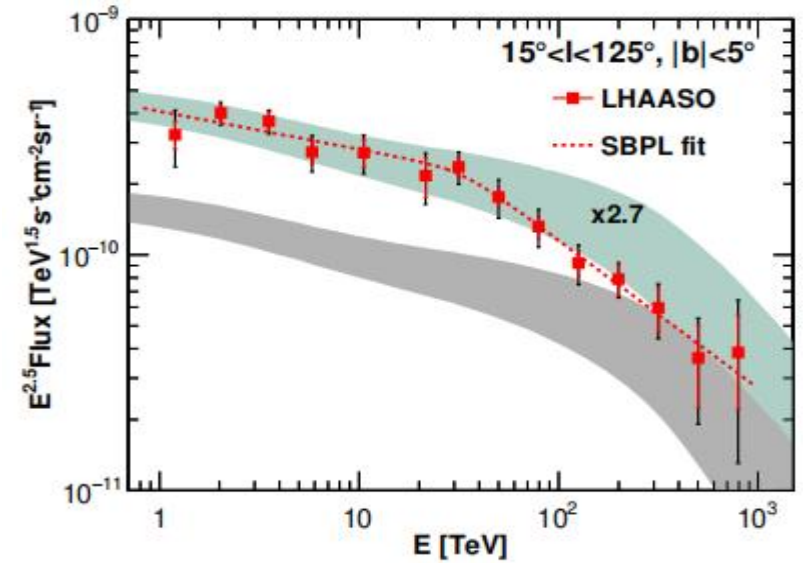
Preliminary!

Preliminary!

# Summary

- The diffuse emission from 1 TeV to 1 PeV from the Galactic plane was observed with high significance; Firstly detected in the outer Galaxy region!
- A spectral break around 30 TeV is found in the inner region, with a change of indices by  $\sim 0.5$
- The longitude distribution deviates from gas distribution; there is possible spectral variation of the spectra across the Galactic plane
- Together with Fermi-LAT, the wide-band data show excesses from several GeV to 10s TeV compared with a traditional CR propagation model, which could be explained by a population of unresolved sources (pulsar halos or secondary interaction at source)

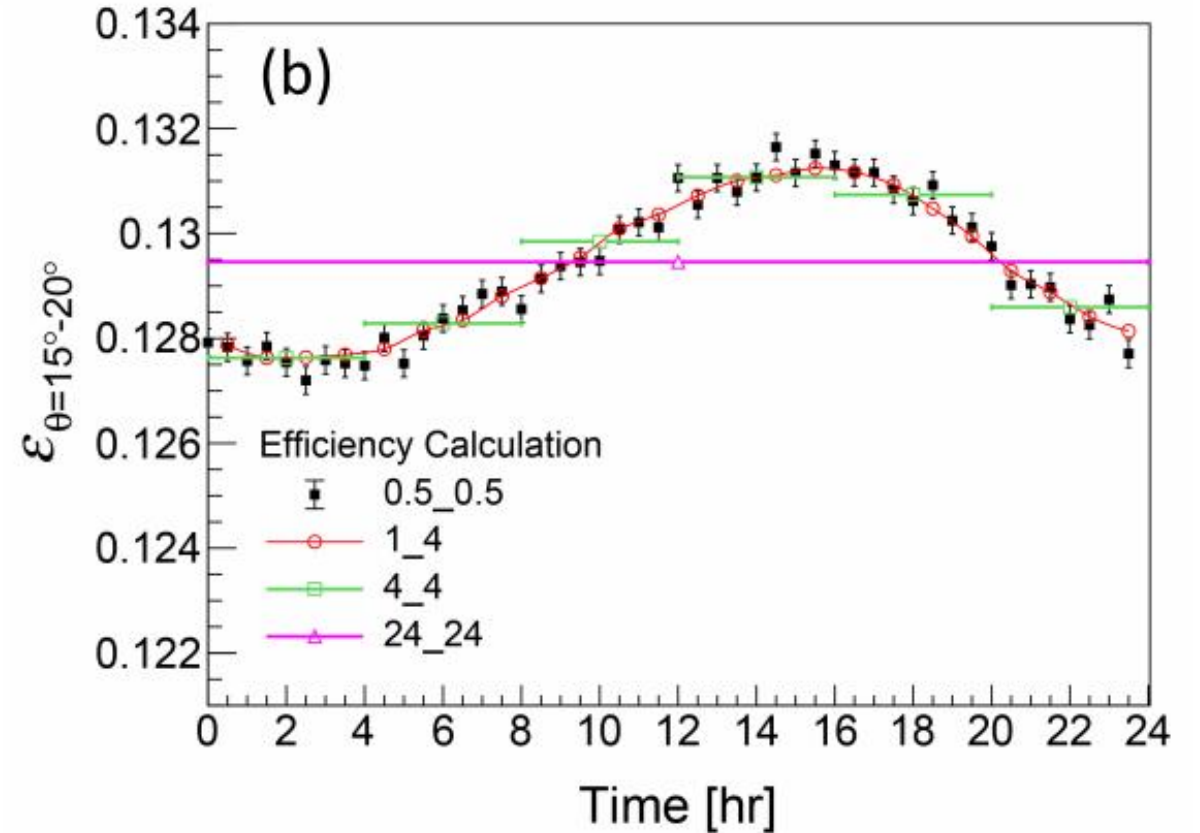
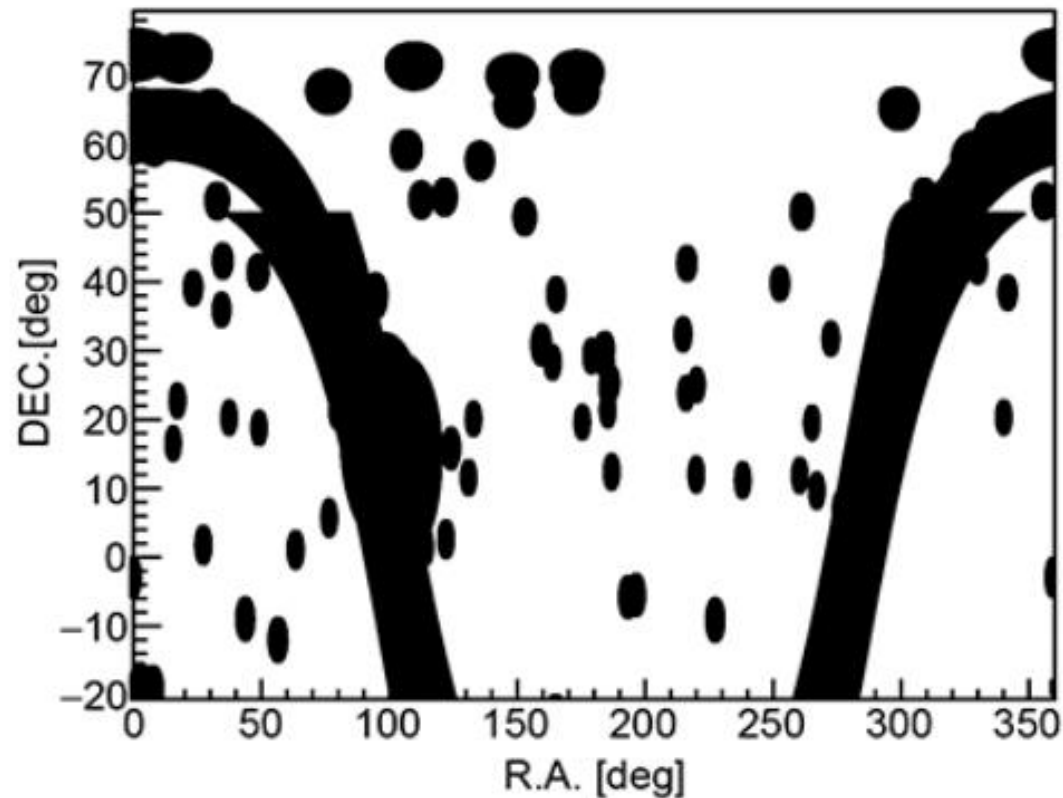
# Thank you!







# Background estimate



- Direct integral method: assuming the spatial distribution in detector coordinate is stable in a reasonably short time bin
- Efficiencies do vary slightly with time, and thus a sliding window method is adopted (1\_10 is used as benchmark, 1 hr step and +/-5 hr window)

# Residual source contamination

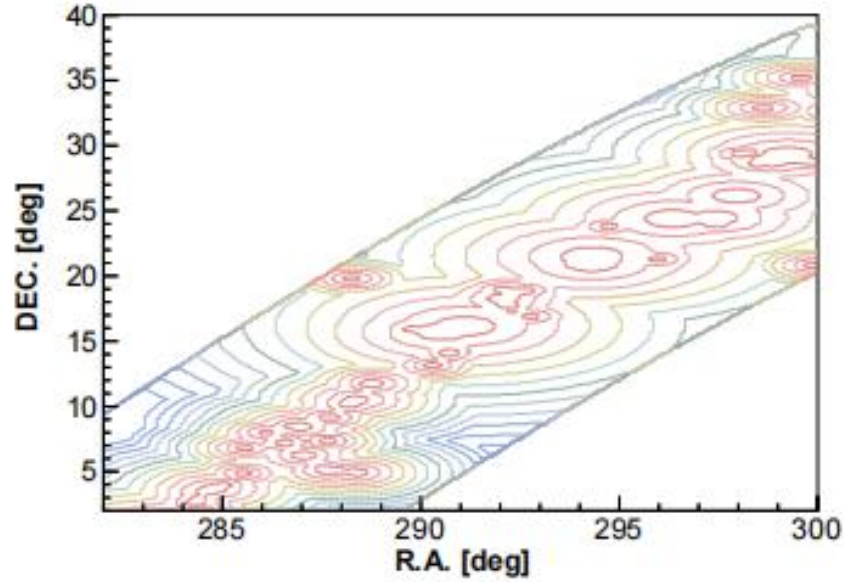


TABLE S1. Residual fractions of resolved sources to the total signal in different hit bins.

$N_{\text{hit}}$	Inner Galaxy (%)	Outer Galaxy (%)
60-100	$11.12 \pm 0.19$	
100-200	$4.97 \pm 0.12$	
200-300	$3.76 \pm 0.18$	$1.57 \pm 0.10$
300-500	$3.36 \pm 0.21$	$1.10 \pm 0.09$
500-800	$3.07 \pm 0.31$	$1.18 \pm 0.20$
>800	$2.75 \pm 0.49$	$1.86 \pm 0.33$

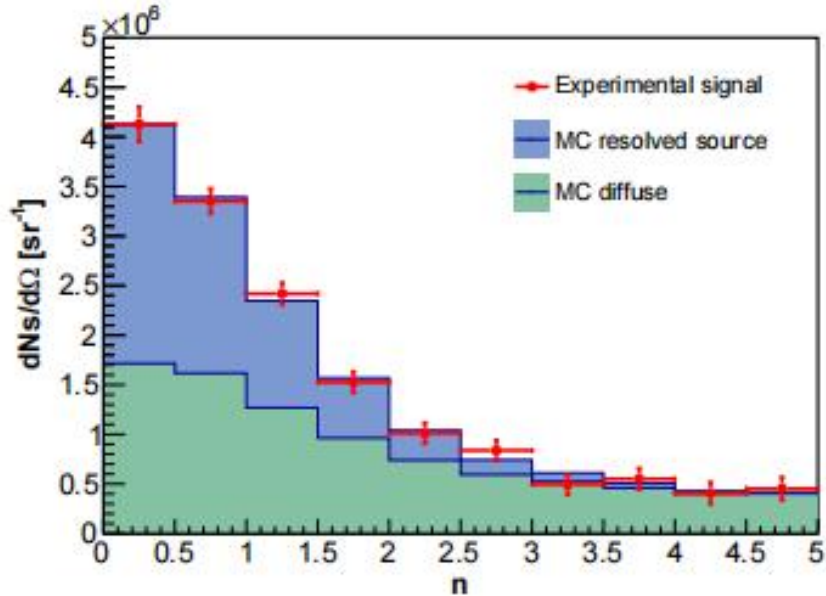


Table 5: Proportion (%) of contamination ( $f_{\text{cont}}$ ) of residual sources (LHAASOCat+TeVCat) to the DGE.

$\log_{10}\left(\frac{E_{\text{rec}}}{\text{TeV}}\right)$	Inner Galaxy region			Outer Galaxy region		
	$n = 2.0$	$n = 2.5$	$n = 3.0$	$n = 2.0$	$n = 2.5$	$n = 3.0$
1.0-1.2	$11.37 \pm 1.09$	$5.97 \pm 0.67$	$3.56 \pm 0.51$	$9.55 \pm 3.03$	$4.58 \pm 1.63$	$2.65 \pm 1.22$
1.2-1.4	$8.77 \pm 0.71$	$4.26 \pm 0.43$	$2.42 \pm 0.31$	$5.45 \pm 1.00$	$2.25 \pm 0.44$	$0.98 \pm 0.20$
1.4-1.6	$8.14 \pm 0.73$	$2.97 \pm 0.36$	$1.37 \pm 0.22$	$4.32 \pm 0.66$	$1.39 \pm 0.23$	$0.49 \pm 0.09$
1.6-1.8	$6.66 \pm 0.56$	$1.95 \pm 0.21$	$0.76 \pm 0.11$	$6.07 \pm 1.30$	$1.88 \pm 0.45$	$0.58 \pm 0.15$
1.8-2.0	$6.56 \pm 0.70$	$1.97 \pm 0.27$	$0.87 \pm 0.16$	$2.44 \pm 0.45$	$0.77 \pm 0.16$	$0.22 \pm 0.05$
>2.0	$3.26 \pm 0.23$	$0.76 \pm 0.06$	$0.20 \pm 0.02$	$1.47 \pm 0.34$	$0.39 \pm 0.09$	$0.10 \pm 0.03$

At 100 GeV, the data is about  $4 \times 10^{-3}$ , when subtracting sources (yellow) and IGRB (brown), the result is about  $3 \times 10^{-4}$ , which is about 2 times of the GDE model (blue) of  $1.5 \times 10^{-3}$

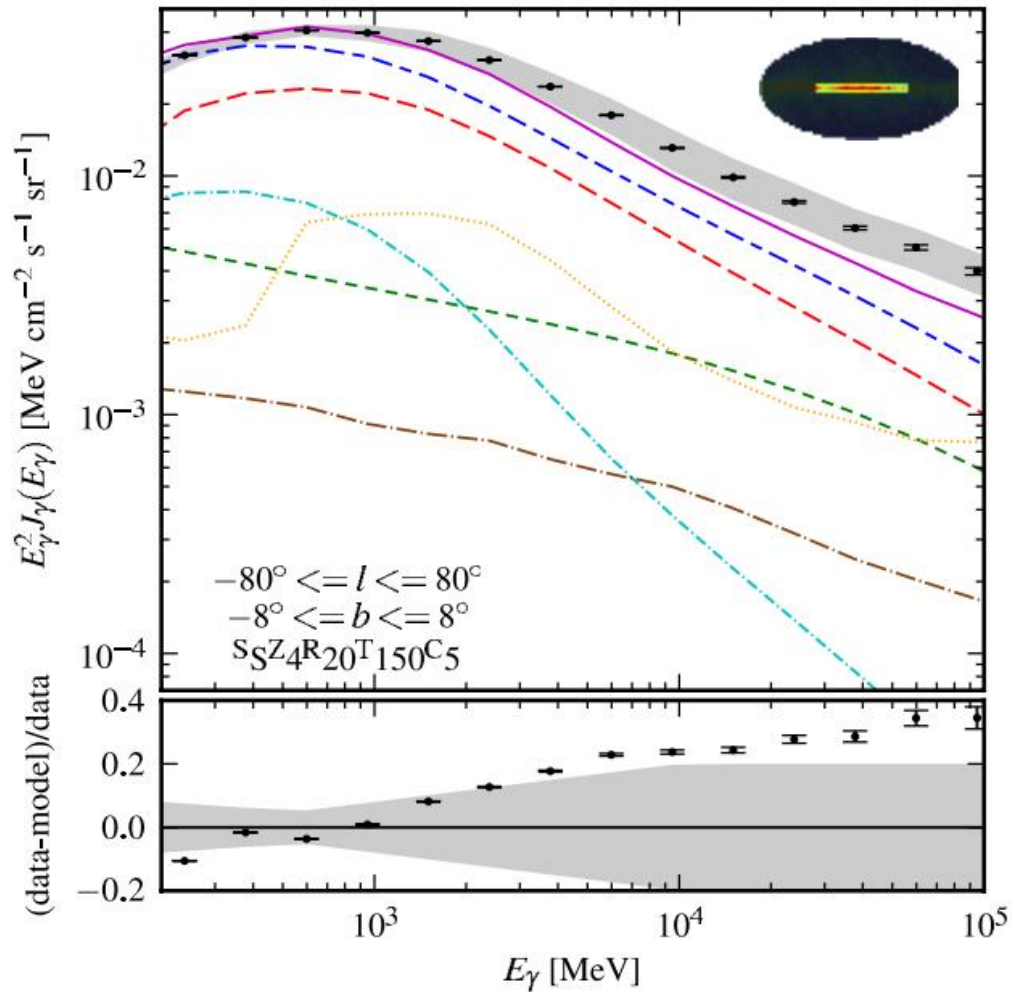
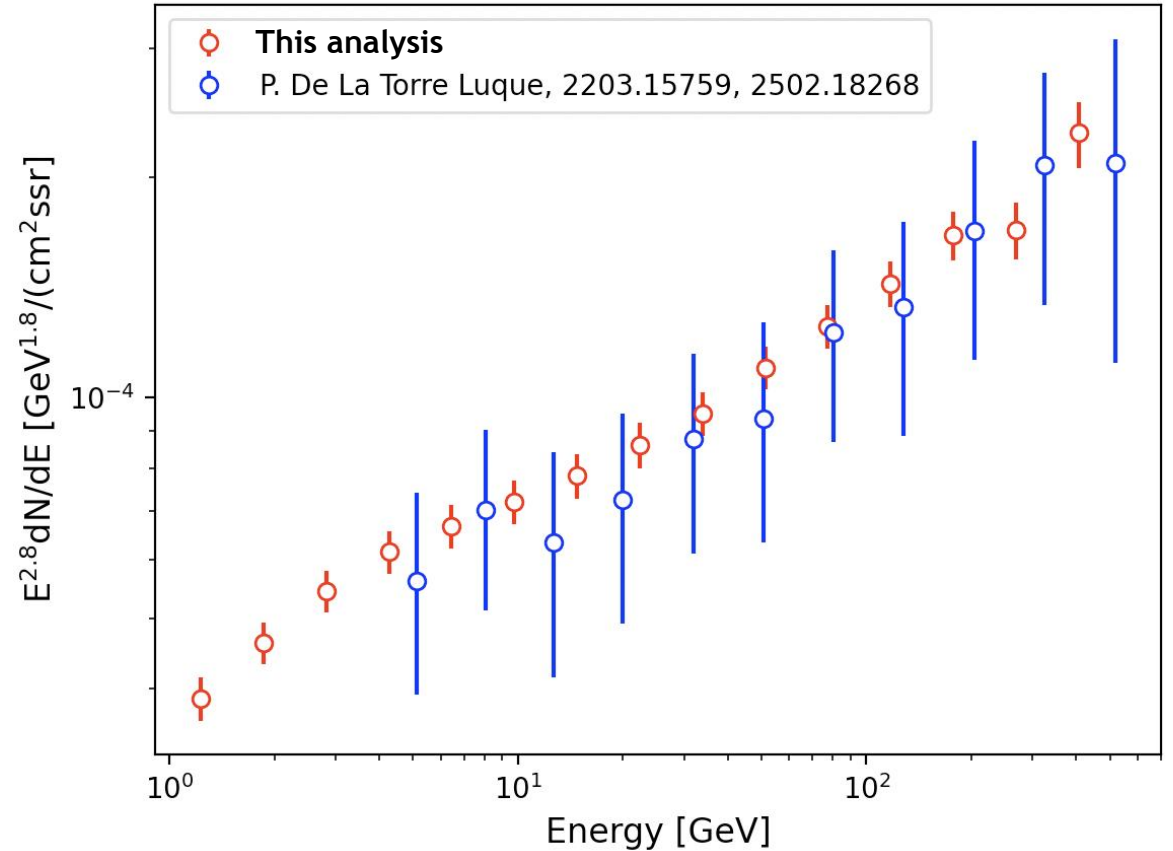


Fig. 17 of Ackermann et al. (2012)



25 < l < 100, -5 < b < 5, no mask